Malaysian Journal of Energy and Applications 1 (2026): 24-56
https://doi.org/10.17576/myjea.2026.01.24

SYSTEM ANALYSIS OF CONVENTIONAL DMFC VERSUS MEMBRANE-LESS FUEL CELL: ELECTRODE ARCHITECTURE

Iesti Hajar Hanapi[1]*, Siti Kartom Kamarudin[1,2]*, Norazuwana Shaari[1] & Siti Hasanah Osman[1]
[1] *Fuel Cell Institute, Universiti Kebangsaan Malaysia, 43600 UKM Bangi, Selangor, Malaysia.*
[2] *Department of Chemical Engineering, Universiti Kebangsaan Malaysia, 43600 UKM Bangi, Selangor, Malaysia.*

**Corresponding author: ctie@ukm.edu.my; iestihajar@gmail.com*

Received 19/6/2026; Received in Revised Form 22/6/2026;
Accepted 22/6/2026; Available Online 20/07/2026.

Abstract

Direct methanol fuel cells (DMFC) are increasingly recognized as a promising energy conversion technology, particularly suited for compact and portable power applications, owing to the high energy density and simple fuel management. In traditional DMFC, the fundamental electrochemical unit is the membrane electrode assembly (MEA), which consists of a proton-conducting membrane sandwiched between the anode and cathode electrodes. Alternatively, the development of membrane-less DMFC systems, which employ a co-laminar microfluidic flow to establish a "virtual membrane," eliminates the necessity for a physical membrane while still facilitating proton transport and electrochemical separation. Electrodes continue to be a critical element in both systems, as they regulate the efficacy of methanol oxidation and oxygen reduction reactions, despite the architecture differences. The present review critically evaluates the present state and prospective trajectory of electrode development in both conventional and membrane-less DMFC. Engineering electrodes that provide improved catalytic activity, structural durability, and mass transport characteristics while adhering to a variety of operational constraints is the primary challenges. This paper provides a comparative analysis of the progress and limitations in each system by investigating the fundamental operating principles and reviewing recent innovations in electrode materials, and architectures. The investigation also investigates the operational stability, scalability, and performance trade-offs that are linked to real-world deployment. The review emphasizes the direct relationship between advancements in electrode technology and global sustainability initiatives, as they are consistent with the United Nations Sustainable Development Goals SDG 7 (Affordable and Clean Energy) and SDG 13 (Climate Action).

Keywords: Direct methanol fuel cell (DMFC), Membrane-less fuel cell, Electrode architecture, Microfluidic fuel cell, Laminar flow fuel cell (LFFC)

1.0 Introduction

The increasing global population has intensified global apprehensions regarding the necessity of additional energy in the daily marketplace. Malaysia's economic prosperity is significantly influenced by its production of hydrocarbons and fossil fuels. The Renewable Energy Policy was implemented in Malaysia with the objective of achieving a 9% renewable energy component in the nation's total energy blend by 2020 [1]. Malaysia has the capacity to address environmental concerns on a local, regional, and global scale by implementing renewable energy sources, such as fuel cells. This is appropriate for the nation, as Malaysia is dedicated to the promotion of renewable energy and has reaffirmed its objective of achieving a 20% share of renewable energy in its energy generation by 2025 [2]. The conversion of chemical energy

into electrical power is a cornerstone of modern infrastructure, spanning applications from megawatt-scale utility plants and kilowatt-scale electromobility to watt-scale portable electronics. To facilitate these energy transitions, various electrochemical and mechanical conversion technologies have been engineered, including electric generators, batteries, and fuel cells. Unlike closed-loop storage systems, fuel cells function as open thermodynamic systems characterized by continuous electrochemical oxidation and reduction. By utilizing steady-state reactant streams—typically hydrogen and oxygen—these devices maintain a sustained reaction flow, enabling the efficient and simultaneous generation of electricity and thermal energy [3].

Fuel cells offer significant advantages for portable power applications due to their high energy density, long operational life, simple design, and cost-effectiveness [4]. Currently, proton exchange membrane fuel cells (PEMFC) and direct methanol fuel cells (DMFC) represent two of the most developed types of low-temperature fuel cells [5]. According to a multitude of researchers, DMFC is regarded as a highly prospective and suitable solution for portable devices in order to address the impending energy crisis [6]. This is attributed to their ability to operate at low temperatures, high energy conversion efficiency, and minimal pollutant emissions [7]. Due to its affordability, ubiquitous availability, convenient storage and handling, and renewable nature, the methanol fuel is an appealing option [8].

The MEA is composed of gas diffusion layer (GDL), catalyst layer (CL), and polymer electrolyte membrane (PEM) [9]. Nevertheless, the membrane's presence elevates the likelihood of fuel crossover, which results in catalyst toxicity and an overall decrease in performance due to the reduced active surface area. Furthermore, membrane fabrication presents substantial obstacles due to its high cost and high level of complexity [10]. Consequently, researchers are conducting research on membrane-less fuel cells to resolve these concerns and eliminate the necessity for PEM. Membrane-less or microfluidic fuel cells demonstrate potential for low-power one-chip devices [11], which are suitable for lab-on-a-chip devices with variable power consumption requirements [12]. The membrane-less fuel cell system is capable of recharging secondary batteries. Abrego Martinez [13] conducted a study on the design of a 2-cell stack for devices with minimal power consumption, including LED lighting, blood diagnostics, microanalytical systems, and DNA analysis devices [14,15]. The attainment of a high-power density in microfluidic devices continues to be a substantial obstacle. Electrode research is considered a viable method for improving the efficacy of both conventional systems and membrane-less fuel cells.

Particularly in the electrochemical reactions involving the oxidation and reduction processes is significantly impacted by the electrode modifications. Several authors have investigated critical components of DMFC electrode technology. Zainoodin et al. [16] have disclosed the application of nanotechnology, Ramli et al. [17] have reviewed nanocatalysts and their obstacles, and Ke et al. [18] have investigated the structural and functional properties, applications, preparation methods, and design mechanisms of non-carbon support materials. The temporal evolution of research output in the field of DMFC and membrane-less fuel cells is depicted in Figure 1. The number of publications related to DMFC experienced a significant increase in the early 2000s, and it reached a zenith between 2010 and 2014. Subsequently, there was a gradual decline, but interest in the field persisted until 2024, as illustrated in Figure 1 (a). The growth pattern in Figure 1 (b) is consistent with a more focused trend on electrode development within DMFC, which suggests the critical role of electrode architecture in enhancing fuel cell performance. On the other hand, membrane-less fuel cell research (Figure 1 (c)) began to emerge after 2002, with a consistent increase in publications that reached a climax around 2015. This reflects the increasing interest in low-cost, simplified fuel cell systems that are appropriate for microscale and portable applications. The field is still evolving and has significant potential for innovation, as evidenced by the progressive increase in

membrane-less systems that focused on electrode development (Figure 1 (d)), which peaked more recently around 2020. This analysis of trends underscores the ongoing global research interest in both conventional and membrane-less fuel cell technologies, with a particular emphasis on the crucial role of electrode design and optimization in performance improvement. It further substantiates the relevance and timeliness of a comprehensive review that contrasts and evaluates the electrode architectures of these two fuel cell systems.

Figure 1. Temporal Evolution research of (a) direct methanol fuel cell that (b) focusing on electrode development and (c) membrane-less fuel cell that (d) focusing on electrode development.

Tables 1 and 2 provide a thorough description of recent research on both conventional and membrane-less DMFC. While existing literature frequently isolates catalyst material synthesis or macro-scale microfluidic channel geometries as primary performance drivers, such perspectives often overlook the critical intermediary role of the electrode architecture. The spatial configuration, porosity gradient, and structural topology of the electrode govern the localized multi-phase mass transport (liquid methanol and gaseous CO_2) and charge transfer kinetics that ultimately limit both systems.

The fundamental research gap this review addresses is not merely a lack of comparative literature, but a distinct engineering divergence in how electrode architectures manage internal system inefficiencies:

- In Conventional DMFCs: The electrode architecture (specifically the gas diffusion layer topology and catalyst layer thickness) serves as the primary physical barrier controlling the trade-off between local methanol mass transport and adverse methanol crossover across the polymer electrolyte membrane.
- In Membrane-less DMFCs: In the absence of a physical membrane, system stability relies entirely on laminar flow dynamics. Here, the electrode architecture must be engineered to maintain a stable electrochemical boundary layer, preventing fuel-oxidant mixing without introducing excessive parasitic pressure drops.

Therefore, optimizing the intrinsic activity of a catalyst material or refining bulk microfluidic flows is insufficient if the underlying electrode architecture fails to facilitate efficient multi-phase transport or boundary layer control. This paper provides a targeted, comparative

investigation of these architectural technologies across both traditional and membrane-less DMFCs, guided by three main objectives:

1. To trace the evolution of structural electrode designs—such as 3D porous frameworks, gradient porosities, and integrated gas-evolving topologies—tailored to the distinct mass-transport and crossover demands of both systems.
2. To bridge a critical knowledge gap by establishing the first direct comparative evaluation of how architectural principles from membrane-less configurations (e.g., boundary-layer control) can inform the mitigation of crossover in conventional systems, and vice versa.
3. To align next-generation electrode manufacturing strategies with global sustainability metrics, specifically SDG 7 (Affordable and Clean Energy) and SDG 13 (Climate Action), by emphasizing scalable, low-loading, and binder-free architectural designs.

By shifting the analytical focus from isolated material properties to integrated systemic architectures, this review aims to provide a predictive framework for researchers designing high-efficiency, commercially scalable DMFC technologies.

Table 1. Related review of the electrode for conventional DMFC

Year	Ref.	Summary
2021	[19]	This review critically evaluates the various factors that cause degradation in the MEA of conventional DMFC, which is essential for improving the reliability and efficiency of these fuel cells.
2024	[20]	This paper introduces and experimentally validates a new MEA design with a double-layered catalyst to enhance the performance of micro-DMFC by improving current distribution and reducing fuel crossover.
2022	[21]	This review explores the use of nanostructured conducting polymer-based supports for developing anode materials, highlighting their importance in lowering catalyst usage and supporting the commercial development of DAFC
2018	[22]	This review presents an overview of the methanol electrooxidation process and its underlying mechanisms on Pt and Pt-based catalysts in acidic media, focusing on catalyst size and morphology affect to the electrocatalytic performance.

Table 2: Related review for membrane-less fuel cell

Year	Ref.	Summary
[23]	2024	This paper gives insight into the computational modelling study of membrane-less fuel cell system including governing equation, the configuration of the existing systems, and studies of operational condition.

[24]	2022	This paper focuses on the recent development of paper-based membrane-less fuel cell system that invented in 2014. The fundamental, fabrication method, the geometrical design and its performance also being discussed in this work. Besides, the scale up of the system also being addressed with the future perspective to improve the performance of the system.
[25]	2021	Significant recent research efforts involving the membrane-less fuel cell classification based on reactant, flow configuration, and electrode structure. Additionally, the different types of fuel were detailed discussed in this paper including the stacking development of the system.
[26]	2021	This review article specifically focuses on the microchannel geometry, as well as the architecture and arrangement of electrodes within membrane-less fuel cell system.
[27]	2021	This paper outlines the six categories of flow configurations in membrane-less fuel cell system that reported in 2002 to 2020 that highlight on the factors that affecting the power density by modify the diffusive mixing and depletion zones.
[28]	2019	This work compares various channel shapes (Y-, T-, F-, H-, bridge-, and orthogonal), which strongly affect fuel mixing and power output. It also discusses easy fabrication techniques (CNC micromilling, soft/photolithography, and paper-based methods).
[29]	2018	Focus on the catalyst-selective strategy for the membrane-less fuel cell system.
[30]	2018	These papers addressed the membraned and membrane-less microfluidic microbial fuel cell system and its roadmap of the challenges and the opportunities for the development of this technologies.
[31]	2017	This article provides an analysis of key scientific research on enzyme fuel cells, with a focus on common challenges such as low cell voltage, limited current density, durability concerns, electrode development, device design, and system modelling.

2.0 Fundamentals of DMFC

The conventional and membrane-less DMFC system is the primary focus of this research. Conventional DMFC systems utilize liquid fuel for oxidation at the anode and air or oxygen vapor for the reduction process at the cathode. The electrons traverse an external circuit, while the ions traverse the electrolyte membrane. The conventional DMFC is capable of operating in either an acidic or alkaline environment, contingent upon the specific electrolyte used in the system. Figure 2 (a) and (b) illustrate the reaction that transpires in acidic and alkaline DMFC. The kinetics of alcohol oxidation in acidic conditions are more complex than in alkaline conditions [32].

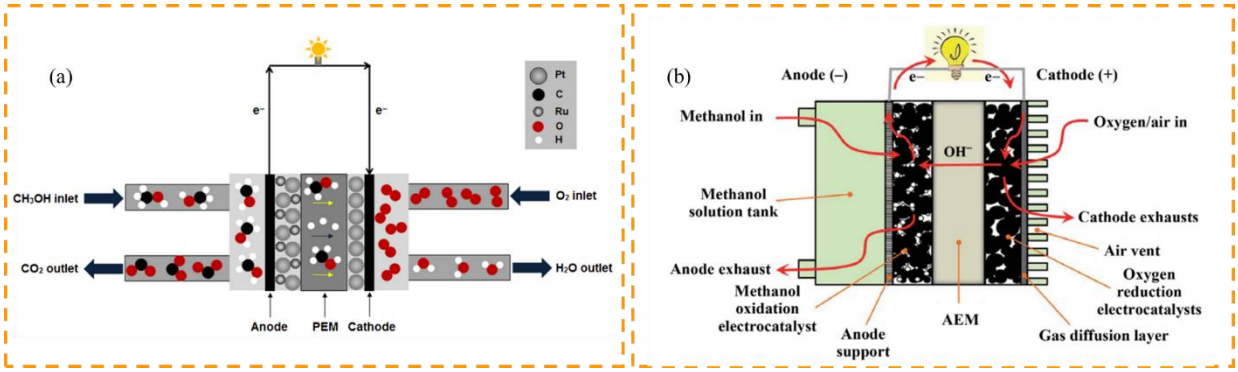

Figure 2. The working principle of (a) acidic [33] and (b) alkaline media DMFC system [34]

Perfluorosulfonic acid is commonly utilized as the electrolyte membrane in DMFC systems operating in acidic environments. In an acidic environment, methanol undergoes electrocatalytic oxidation at the anode, producing protons, electrons, and carbon dioxide as depicted in Figure 2. The protons are conducted to the cathode via the proton exchange membrane (PEM), while the electrons flow through an external circuit to generate electrical power. Oxidation occurs at the anode and reduction of oxygen at the cathode in acidic environments, as indicated by Equations (1) and (2), with Equation (3) representing the overall reaction.

Anode:

$$CH_3OH + H_2O \rightarrow CO_2 + 6H^+ + 6e^- \qquad 0.016\ V \qquad \text{eq. (1)}$$

Cathode:

$$\frac{3}{2}O_2 + 6e^- + 6H^+ \rightarrow 3H_2O \qquad 1.229\ V \qquad \text{eq. (2)}$$

Overall

$$CH_3OH + \frac{3}{2}O_2 \rightarrow CO_2 + 2H_2O \qquad 1.213\ V \qquad \text{eq. (3)}$$

Researchers have investigated a variety of solutions to the primary challenge of fuel crossover in DMFCs, which is the migration of fuel through the membrane. Cai et al. [35] discovered that polymer nano-sieves with narrow apertures effectively prevented methanol crossover at low concentrations. The power density of 132 mW cm^{-2} was achieved by stable phosphotungstic acid (HPW) self-anchored hybrid membranes (PES/PVP-HPW) that were developed by Xu et al. [36]. Additionally, You et al. [37] conducted an investigation into an alternative to Nafion by introducing composite membranes composed of sulfonated polyimide (SPI) and rice husk ash (RHA). These membranes achieved a peak power density of 13.0 mW cm^{-2}.

On the other hand, alkaline DMFC technology uses the same principle as DMFC, but with an alkaline environment and an alkaline anion exchange membrane (AEM) to exchange OH− as can be seen in Figure 2 (b) and Eq. (4) to Eq. (6) [38]. Electrochemical reactions in alkaline media are kinetically favoured over protonic ones due to OH− at the anode that accelerate MOR and carbonate and bicarbonate leaks in the outlet [39]. Furthermore, alkaline environments exhibit lower corrosiveness compared to acidic environments, enabling the

use of non-precious metal catalysts for methanol oxidation reaction (MOR) and oxygen reduction reaction (ORR) with enhanced durability [40]. In addition, the utilization of alkaline electrolytes enhances the longevity of the fuel cell components. Indeed, optimizing alkaline fuel concentrations offers a simpler approach to mitigate issues such as bipolar plate degradation [41], carbon support dissolution [42], and anodic catalyst leaching [43].

DMFC employing anion exchange membranes (AEM) present a promising solution to these limitations. This is due to several factors: firstly, they offer improved electrode kinetics and catalyst stability, enabling the use of more cost-effective non-noble metal catalysts. Secondly, the transport of hydroxide ions in the opposite direction helps reduce crossover. Lastly, AEM-based DMFC exhibit better water management [44,45]. For instance, Sajjad et al. [46] utilized a guanidinium blend AEM, achieving a power density of 2.0 mW cm^{-2} and an OCV of 0.69 V. Similarly, Gupta et al. [47] reported an OCV of 0.6 V and a power density of 7.1 mW cm^{-2} using a MEA based on KOH-doped PVA AEM. Varcoe et al. [48] demonstrated impressive results with a peak power density of 2.8 mW cm^{-2} employing a poly(ethylene-co-tetrafluoroethylene)-based AEM.

Therefore, it can be concluded that the inclusion of KOH in the fuel is essential to boost the power densities. This is because the high concentration of OH^- ions enhances conductivity and efficient electrode reactions. Burhan et al. [49] tested Fumasep® membrane (FAA3-50) in methanol and KOH solutions, achieving 5.2 mW cm^{-2} at 60 ◦C and 33.2 mW cm^{-2} at 80 ◦C peak power density. Besides, Zakaria et al. [50], the QPVA - based membrane can achieve an ionic conductivity of 1.08×10^{-2} S cm^{-1}, yielding a maximum power density of 6.92 mW cm^{-2}. This surpasses the performance of a Nafion - doped KOH membrane, which produces only 5.09 mW cm^{-2}. The author continued the study of relation between the effect of different doped KOH concentrations inside the membranes resulted a power density of 11.28 mW cm^{-2} when exposed to 2 M of KOH [51]. The Table 3 shows the previous studied of DMFC system for acidic and alkaline media.

Anode:

$$CH_3OH + 8OH^- \rightarrow CO_3^{2-} + 6H_2O + 6e^- \qquad \text{-0.810 V} \qquad \text{eq. (4)}$$

Cathode:

$$\frac{3}{2}O_2 + 6e^- + 3H_2O \rightarrow 6OH^- \qquad \text{0.401 V} \qquad \text{eq. (5)}$$

Overall

$$CH_3OH + \frac{3}{2}O_2 + 2OH^- \rightarrow CO_3^{2-} + 3H_2O \qquad \text{1.211 V} \qquad \text{eq. (6)}$$

The electrochemical conversion concept of conventional fuel cells is also applicable to membrane-less, or microfluidic DMFC as presented in Figure 3 (a) and (b). Microfluidics is referring to the investigation fluid flow and transport processes within microscale structures, typically characterized by at least one dimension between 1 and 1000 μm [52,53]. A parallel co-laminar flow is generated when two laminar streams of fluids with comparable viscosity and density travel through a microchannel, which is also referred to as a co-laminar fuel cell (LFFC). The primary distinction is the replacement of the PEM role with a mixing zone that enables the passage of ions across the channel, which is referred to as the "virtual membrane"

or "diffusion zone." The system generates a "virtual membrane" as a result of co-laminar fluxes, which facilitate the transportation of protons. Conversely, the electron is directed across the burden to generate electricity. The Table 4 represent the advantages and disadvantages of the membrane-less fuel cell system.

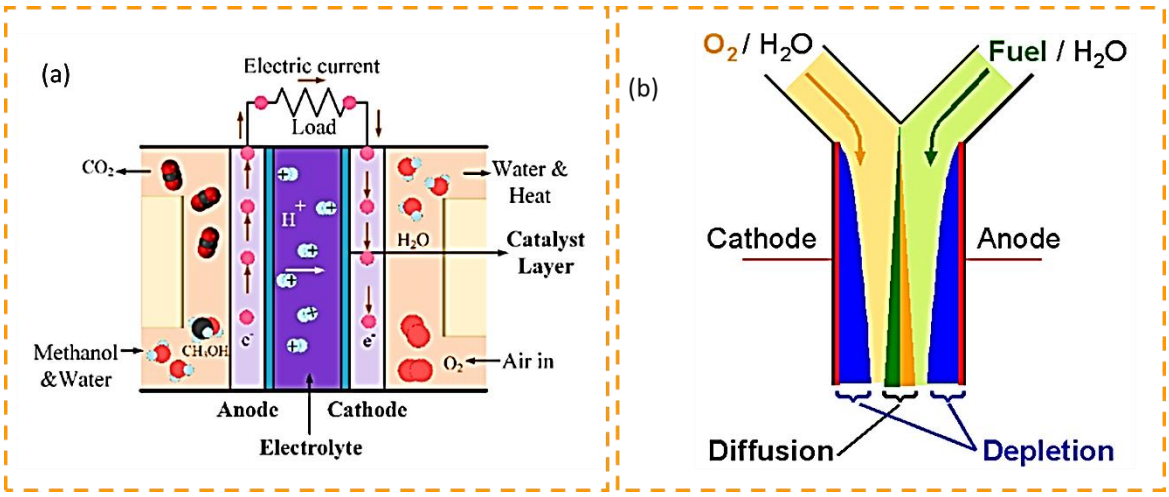

Figure 3. The working principle of the (a) conventional DMFC [54] and (b) membrane-less system [55]

The anolyte and catholyte streams flow along the microchannel after being introduced separately through various inlets. Initially, liquid anolyte and catholyte were introduced into the inlets at specific flowrates to maintain a Reynolds number below value 2100 [56]. Hanapi et al. [57] reported that the Reynolds number for the developed system is approximately to 24. Additionally, as demonstrated in Figure 4, Cohen et al. [58] used a visualising technique to ascertain the laminar flow by means of bathophenanthroline sulphonate (BPS) and $FeCl_2$. The chemicals will form a reddish-cherry solution when there is mixing in the reactants, nevertheless, the channel region at the point of contact did not exhibit any coloration.

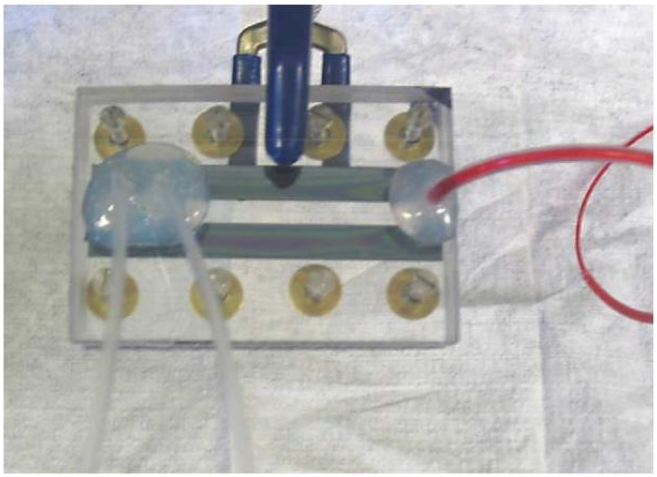

Figure 4. Visual analysis of laminar flow determination for membrane-less fuel cell [58]

Since the membrane-less fuel cell system employs liquid electrolyte, it can be designed to operate with several types of media. For example, an acid medium can be used in the cathode while an alkaline medium can be used in the anode, or vice versa. The use of dual-electrolyte media can enhance the OCV of the system without affecting its operational complexity as

presented in eq. (7) until (12). Choban et al. [59] conducted a study on the media flexibility reported a dual-electrolyte medium, commonly referred to as a mixed medium, attains an OCV up to 1.4 V and a power density of 12.0 mW cm^{-2}. The neutralisation process of OH^- and H^+ occur at the liquid-liquid interface or reactants. Based on the eq. (9) and (12), it is noted that the acidic anode and alkaline cathode media have low theoretical OCV. Most of the energy generated from oxidation reduction is by the process of water ionisation. The interaction of galvanic and methanol electrolytic reactions in this configuration has been identified as the cause of the inability to produce significant amounts of energy [60,61].

Therefore, the use of alkaline anode and acidic cathode widely used by the researcher for better performance. Ponmani et al. [60] conducted a study with dual electrolyte media produced 1.81 V OCV. Hanapi et al. [57] investigated the optimization of mixed reactants and oxidants in membrane-less DMFC, achieving a power density of approximately 30 mW cm^{-2}. Table 5 presents previous research on membrane-less fuel cell systems and their performance. Moreover, Chen and the team [62] conducted a computational fluid dynamics (CFD) analysis discovered that the type of electrodes are important for determining the system's performance. The difference of electrode development studies in the conventional and membrane-less DMFC were discussed in the next section. Additionally, the geometrical design of the membrane-less fuel cell system can be found in different shapes and sizes based on the electrode placement [63]. The electrode architecture for the conventional and membrane-less DMFC will be discussed in the next section.

Mixed-media: acidic anode, alkaline cathode

Anode:

$2CH_3OH + 2H_2O \rightarrow 2CO_2 + 12H^+ + 12e^-$ 0.02 V eq. (7)

Cathode:

$3O_2 + 6H_2O + 12e^- \rightarrow 12OH^-$ 0.04 V eq. (8)

Overall:

$2CH_3OH + 3O_2 + 8H_2O \rightarrow 2CO_2 + 12OH^- + 12H^+$ 0.38 V eq. (9)

Mixed-media: alkaline anode, acidic cathode

Anode:

$2CH_3OH + 12OH^- \rightarrow 2CO_2 + 10H_2O + 12e^-$ -0.81 V eq. (10)

Cathode:

$12H^+ + 3O_2 + 12e^- \rightarrow 6H_2O$ 1.23 V eq. (11)

Overall

$2CH_3OH + 3O_2 + 12OH^- + 12H^+ \rightarrow 2CO_2 + 16H_2O$ 2.04 V eq. (12)

Table 3: Research on conventional DMFC in acidic and alkaline medium

Fuel/oxidant	Electrode/catalyst support	Membrane	T ℃	Max power density	Ref.
3 M methanol	Pt/MC Pt/HiSPEC 3000	Nafion 115	26	24.5 22.1	[64]
1 M methanol + O2	Pt-Ru/50 wt% MWCNT + 50 wt% graphene Pt-Ru/MWCNT	Nafion 117	80	68 40	[65]
1 M methanol + O2	N-doped FWCNT Pt/C	FAA3		0.78 0.72	[66]
1 M methanol + O2	Pt-Ru/Vulcan Pt-Ru/GNF Pt-Ru/FWCNT	Nafion 115	30	3.5 13.1 20	[67]
6 M methanol + Air	Pt-Ru (CNT-MEA) Pt-Ru (CP-MEA)	Nafion		23.2 16.0	[68]
1 M methanol + O2	Pt/MC Pt/Vulcan	Nafion 212	60	58 44	[69]
3 M methanol + air	Pt/C	NA	70	63	[70]
2 M methanol	Pt/C with carbon buffer layer Pt-Ru Pt	Poly(ethylene-co-tetrafluoroethylene)	50	2.8	[48]
2 M methanol + O2	Pt-Ru/CB Pt-Ru/CNF Pt-Ru/CB + CNF	NA	NA	12.6 18.3 13.2	[71]
10 M methanol+	Pt-Ru	Nafion	NA	15	[72]

		Nafion/graphene monolayer			
3 M methanol + 1 M KOH	Pt	guanidinium-chitosan blend poly-mers	NA	2.0	[46]
1 M methanol + O2	Pt/TiC-CDC Pt/Vulcan XC-72R	Nafion 117	80	50.16 42.58	[73]
4 M methanol + Air	NA	Nafion/G-CNTs	25	41.6	[74]
		Nafion/Vulcan XC-72R		30	
2 M methanol + O2	Pt/C	SPEEK/Sfu (0.5 wt%) SPEEK		103 70	[75]
		Nafion 117		50	

Table 4. Advantages and disadvantages of the membrane-less fuel cell system [28]

Advantages	**Disadvantages**
Media flexibility	Generate lower power density
Reduced cost	Higher Ohmic loss than conventional
Size flexibility	Heavy
Simpler water management	Reduced gravimetric power and energy density
Higher energy density due to the uses of liquid fuel compared with gaseous fuel.	

Table 5. Previous research of membrane-less fuel cell system.

Fuel/oxidant	Electrolyte	Design features	Power density		Ref.
HCOOH/dissolved O2	H2SO4	PdCo supported on carbon nanotubes on anode	1.75		[76]
V2+/VO2	H2SO4	Parallel cell connection	16		[77]
HCOOH/dissolved O2	H2SO4	Carbon supported rutherium chalcogenide as cathode catalyst	1.9		[78]
H2/O2	KOH	Alkaline fuel cell	110		[79]
HCOOH/KMnO4	H2SO4	Bridged shaped	26		[80]
V2+/VO2	H2SO4	Plate-frame flow-through stack	5.8		[81]
V2+/VO2	H2SO4	Chip embedded thin film current collector	90		[82]
V2+/VO2	H2SO4	Porous carbon electrode		25	[83]
HCOOH/air	H2SO4	Air breathing with fuel reservoir	29		[84]
Formic acid/KMnO4	H2SO4	CNx nanofibers as cathode catalyst	3.43		[85]
Hydrogen peroxide (0.75 M) + Sodium hydroxide (0.75 M)	H2SO4	grooved electrodes and with general planar electrodes for	2.80		[56]

3.0 Recent Advances in Electrode Architecture

Basically, there are some distinctions for the conventional and membrane-less fuel cell system based on the electrode architecture. In conventional DMFC, the electrode present either; i) the catalyst directly on the membrane or ii) on the substrate. However, for the membrane-less system, the electrode can be in a) flow over, b) flow-through, and c) air-breathing electrodes. The key differences between conventional and membrane-less DMFC in terms of electrode and MEA design are summarized in Table 6. These types of the electrode architecture will be discussed in the following sub-section.

Table 6. Comparative analysis of electrode and MEA development in conventional and membrane-less DMFC

Aspect	Conventional	Membrane-less
MEA type	Nafion-based (CCM, GDE, integral MEAs)	No membrane; electrode-separated by laminar flow
Electrode configuration	Flat catalyst-coated layers on membrane or GDL	Planar, interdigitated, 3D porous, or flow-through
Performance limitation	Methanol crossover, membrane degradation	Fuel mixing, limited residence time, microchannel constraints

3.1 Conventional DMFC electrode system

There are four components of a conventional DMFC: the endplate, current collector, bipolar plate, and MEA. The MEA which comprises CL, MPL, and membrane, is the primary compartment as previously mentioned. The conventional DMFC system is illustrated in Figure 5 (a) in an exploded view. The electrode development which is a component of the MEA will be the primary focus of this topic. In general, there are two fabrication methods for the electrode or MEA in conventional DMFCs: (i) applying the catalyst layer to the GDL and then hot pressing the two catalyst-coated substrates (CCS) onto a pretreated membrane, and (ii) applying the catalyst layer directly to the pretreated membrane and then combining the catalyst-coated membrane (CCM) [86], as illustrated in Figure 5 (a).

The CCS method, which is favoured for its simplicity and potential for mass production presents challenges related to the interfacial contact between the CL and the membrane [87,88]. The CCS-MEA method typically employs a substrate such as carbon paper or carbon cloth [89]. Additionally, the GDL is essential for the dispersion of reactants across the catalyst layer which in turn improves electron collection and catalyst utilization. Additionally, water flooding which can have a detrimental effect on cell performance is effectively prevented by the GDL. Screen printing, rolling, and spraying are widely used methods for fabricating GDL [90,91]. Lee et al. [92] conducted a comparison of spray coating and screen printing using the preparation procedures detailed in Figure 5 (b), to examine the influence of CL deposition methodology on electrode performance. They discovered substantial disparities in the electrochemical performance and morphology of CL between the two methodologies (Figure 5 (c)). A characteristic of the patterned mesh of the screen was the 23 μm thickness and unidirectional fractures of approximately 100 μm of the screen-printed CL. While mesh rugosity can be an issue with poorly formulated screen-printing pastes, it is frequently

rectifiable through optimization, the fractures observed in Lee et al.'s study resulted in increased voltage drops at high current densities as a result of mass transport limitations. This problem was further exacerbated by the excessive incorporation of phosphoric acid (PA) within the fissures, which exacerbated the opposition to oxygen diffusion [100]. Conversely, the spray-coated CL presented a lumpy surface with grains measuring approximately 50 µm in diameter and no discernible fractures, despite its thinner 16 µm structure. The sprayed CL's superior overall performance was a result of its higher porosity which was advantageous in mitigating PA inundation with respect to the screen-printed CL.

In addition, prior research has shown that the optimal performance of the CCS-MEA is achieved when the second layer of the GDL is present, as it functions as a water-resistant barrier. The incorporation of hydrophobic materials and carbon paper support results in the formation of a substantial aperture volume, which facilitates the transportation of reactants and catalysts. The ultimate performance of CCS-based fuel cells is influenced by these factors [93]. Achmad et al. [94] employed the direct paint method to prepare the MEA achieved a peak power density of 25 mW cm^{-2}. In addition, another study conducted by Zainoodin et al. [95] discovered CCS-MEA utilised three different techniques: direct paint (DP), ultrasonic spraying on the diffusion layer (US - D), and ultrasonic spraying directly on the membrane (US - M). The directly spray on the membrane led to the highest performance due to its ability to minimise ohmic resistance, reduce anode potential, and maximise ECSA as can be seen in Figure 6 (b).

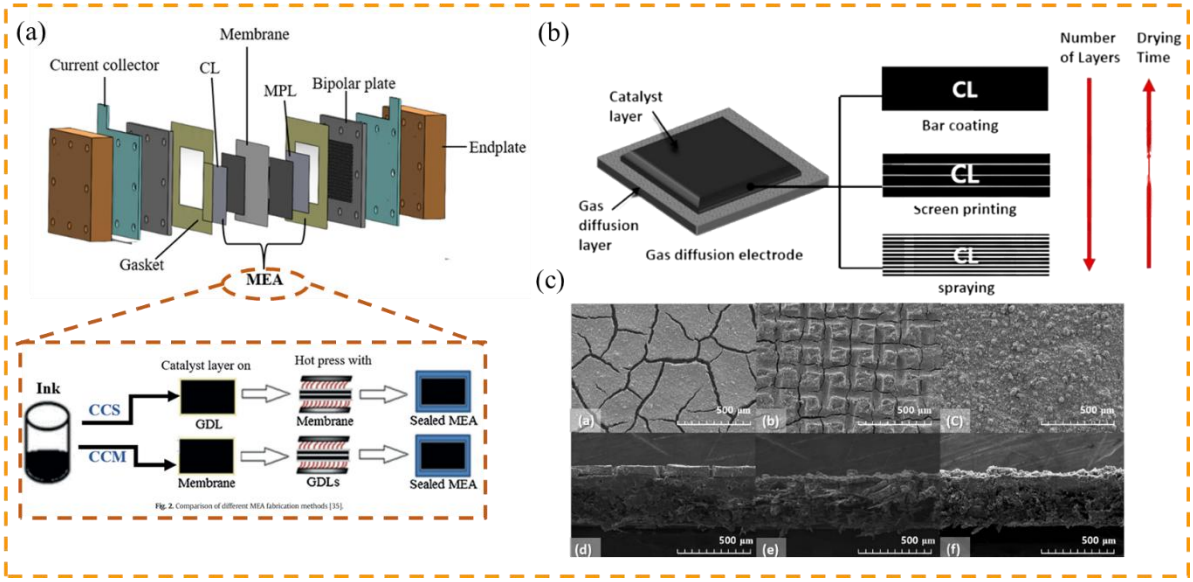

Figure 5. Exploded view of the conventional DMFC with Comparison of different MEA fabrication methods [86], (b))Schematics of the preparation methods for the CL on GDLs by Lee at al.and (c) Top-view and cross sectional SEM images of bar-coated (left), screen-printed (middle), and sprayed CLs (right) [92]

Furthermore, the sputtering procedure has effectively achieved an ultra-low platinum loading for the CCS method, without affecting the cell's performance [96]. The double cathode catalyst layer has been documented as a result of the integration of CCS with the decal method [97]. The inner portion of this layer which is positioned toward the membrane is constructed using the decal method with a Pt loading of 0.3 mg cm^{-2}. The outer portion, which is confronting the gas diffusing layer, is fabricated using the CCS method with a Pt loading of 0.1 mg cm^{-2}. Compared to the MEA generated through the conventional decal method, it resulted in a 13.5% increase in power density.

The other electrode in conventional DMFC is the CCM which have expansion that occurs during the hydration of the membrane can have detrimental effects on the CL in the process of fabricating the CCM [98]. The CCM approach enhanced the contact between the CL and electrolyte membrane resulting in an increase in active sites. This led to a reduction in interfacial resistance and an improvement in the triple phase boundary in the MEA. Shang's team [99] and Su's teams [100,101] both documented the creation of MEA using the CCM technique, by including PA from a pre-doped GDL. It found the CCM-made MEA performed better with low Pt loading than CCS method.

The membrane and catalyst layer facilitate electrochemical reactions, which results in outstanding fuel cell performance and high catalyst utilization efficiency which are advantages of CCM fabrication methods over CCS [102]. Hnat et al. [103] demonstrated that the catalyst burden can be reduced by 75% for CCM-MEA in comparison to CCS-MEA. The CCM-MEA exhibits increased efficiency, power density, and Ohmic and charge transfer resistance. This performance enhancement is primarily attributed to the structural advantages of the CCM-MEA fabrication method, which yields superior catalyst utilization compared to the CCS-MEA configuration at equivalent platinum loadings [104].

The CCM method has several advantages, particularly in terms of performance. However, it also has a drawback that may compromise the long-term performance of the MEA: its brief lifespan. Numerous studies have demonstrated that the MEA fabricated using the CCM method are fragile. It is imperative that additional research be conducted on the CCM fabrication methods to resolve these current issues. Sadeghi et al. [105] investigated the issue of creep behaviour on the CCM, as creep is a form of mechanical degradation that may result in the CCM during fabrication. This factor is important because creep is incontrovertible and is known to diminish the durability of the membrane which in turn deteriorates the system's performance. Nevertheless, researchers have identified solutions to the creep which will inevitably occur and further erode the durability. Therefore, the membrane's durability can be maintained to a certain extent by managing the three primary factors: temperature, relative humidity, and creep stress. Moreover, the catalyst decal method is an enhancement to the CCM approach. For commercial MEA production, the decal method is the most effective, as it involves the coating of catalyst inks on decal substrates, their subsequent curing, and their transfer to a membrane [106]. The decal transfer method was employed by Song et al. [107] to apply thin-film catalyst coatings onto Nafion® membranes in 2005. The resulting power density was more than twice as high as that of the system with conventional MEA. Liu et al. [108] implemented a hybrid approach—direct spraying and a catalyst-coated membrane technique. An efficient CL was effectively generated as a consequence of this innovative approach which involved a heated stereoscopic process.

A lot of research showed that the CCM method outperforms the CCS method. Li et al. [109] used CCS and CCM MEA construction methods for fuel cells and found that CCM performed better. Based on Table 7, CCM-MEA showed lower OCV in all temperatures than the CCS-MEA. Although the CCM-MEA and CCS-MEA used the same electrolyte membrane, spraying catalyst ink onto the membrane surface during preparation could deform the membrane surface due to solvent adsorption, thus increasing crossover. In another study, Rohendi et al. [110] utilized Pt-Co/C by using CCM and CCS method in DMFC and the result can be seen in Figure 6 (c) and (d). These findings are contrary to the other studies as it found that the CCS generated the better performance than CCM.

Table 7. Summary of electrochemical performance (OCV and peak power densities) of CCM-MEA and CCS-MEA with different gas conditions [109].

MEA types	Temperature	Gas condition at anode	OCV/V	Power Density /mW cm-2
CCS-MEA	160	dry	1.000	393
		10% RH	0.994	412
	180	dry	1.02	497
		10% RH	0.992	534
	200	dry	1.020	537
		10% RH	0.997	558
CCM-MEA	160	dry	0.989	500
		10% RH	0.983	526
	180	dry	0.988	598
		10% RH	0.982	613
	200	dry	0.988	614
		10% RH	0.980	617

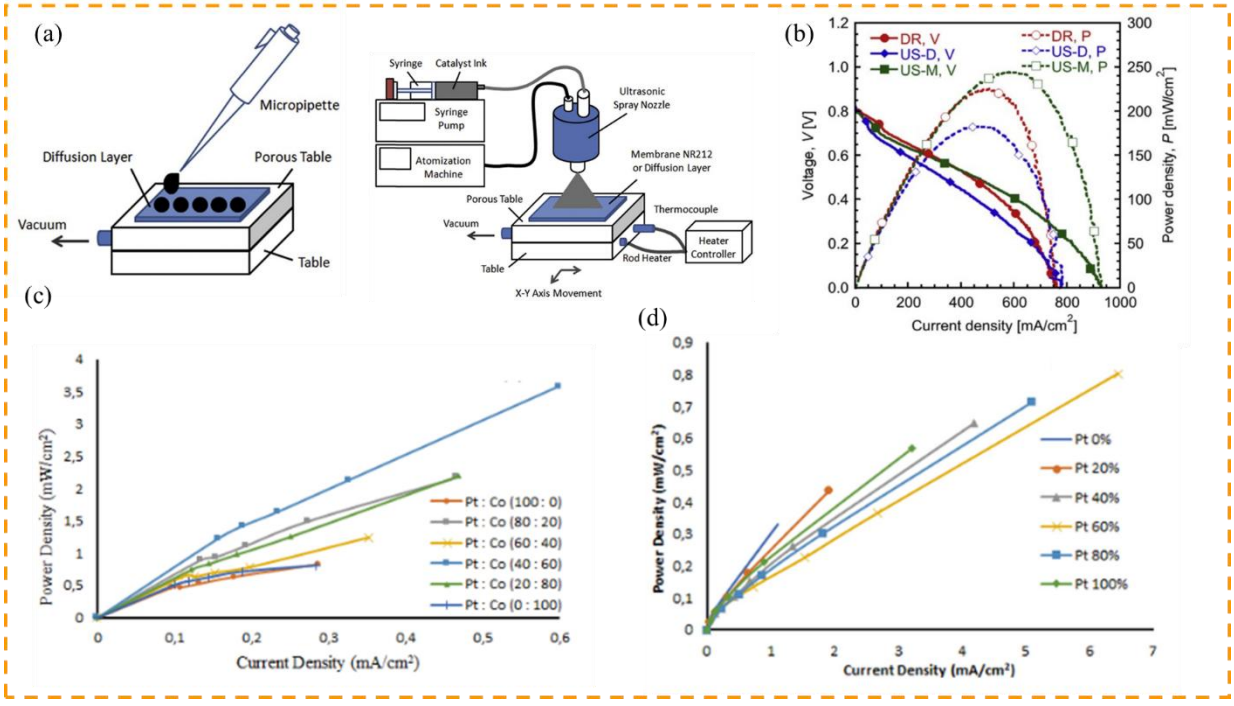

Figure 6. (a) Schematic diagram of the coating techniques of dripping (left) and ultrasonic spraying (right) [95] with (b) Polarization curves of single-cell DFAFCs prepared by the different catalyst layer coating techniques. MEA Performance of electrode with (c) CCS and (d) CCM in DMFC [110]

The conventional electrodes (CCS/CCM) are constructed of Pt/C and ionomer combined in an ink slurry and coated on a membrane or GDL [111]. This process, which starts from the top and moves downwards, generates a randomised structure of electrodes. This structure consists of complex networks of ionomer and pores that hinder the movement of mass and reduce the efficiency of the catalyst [112,113]. Hence, in a recent study by Lee et al. [114] presented the groove electrode, a different type of electrode that offers enhanced performance throughout a broad range of humidity levels with particularly better durability. The process involved creating grooved electrodes by applying a combination of Pt/C and ionomer onto a patterned Si template and then transferring them onto a Nafion membrane.

The CCS and CCM methods employed in MEA fabrication possess significant advantages and disadvantages, as indicated by the preceding discussion. Nevertheless, the primary disadvantage of the CCS fabrication method is the necessity of high Pt loadings to obtain a performance that is comparable to that of the CCM fabrication method. Due to its potential and marketability at low production costs, these factors have persuaded a significant number of researchers to conduct additional research on the CCM fabrication method. Nevertheless, the durability of the MEA is a concern with the CCM fabrication method, rendering the CCS fabrication method the sole viable alternative. The CCS is more challenging to manufacture than the CCM due to the complex technique that necessitates the management of multiple layers of catalysts. Furthermore, membrane wrinkling are not a concern during the CCM fabrication process. Therefore, the CCM fabrication method has the potential to become the primary method for preparing MEA in the future and has undergone numerous enhancements.

3.2 Membrane-less electrode system

The geometric design of membrane-less fuel cell systems is influenced by the varieties and positioning of electrodes, which can be classified as flow-over, flow-through, and air-breathing electrodes [115]. A variety of materials and processing variables must be taken into account when constructing a fuel cell. These include the selection of the carrier substrate for channel formation and the desired geometry, the determination of the catalyst structure and deposition method on the supporting substrate, and the selection of the assembly method for electrodes and channels to facilitate the creation of a liquid-tight sealed cell with interfaces for instrumentation and fuel/oxidant delivery systems.

3.2.1 Flow-over electrode

The flow-over electrodes can be categorized as side-by-side streaming and vertically-layered streaming as portrayed in Figure 7. Ferrigno et al. [116], utilized Y-shaped channel with side-by-side streaming configuration. The monolithic cell design, which integrates microchannels and electrodes within a single layer shows promise for incorporation into on-chip systems [117]. Monolithic design is an appealing approach for this type of system where both electrodes are created on a single substrate [118]. For side-by-side streaming, the vertical fuel-oxidant interface may undergo gravity-induced reorientation, leading to the failure of membrane-less system functioning. The side-by-side streaming have been widely studied for Y- and T-shaped

microchannels [57,80,119]. Whereas the vertically-layered streaming technique employs a multi-layer sandwich construction with electrodes positioned on the sides of the channel. This entire structure is then sealed between two more plates. Moreover, flow-over designs usually entail the continuous flow of anolyte and catholyte over flat electrodes. Due to insufficient convective mass transport, a depletion layer develops over each electrode, resulting in a low reactant concentration. Da Mota et al. [120] attained a power density of 270 mW cm^{-2} using thin film Pt electrodes in a flow-over configuration. Notably, the integration of a staggered herringbone mixer to produce chaotic flow was the sole means to overcome mass transfer restrictions and achieve such a high-power density. Liu et al. [121] proposed a herringbone-shaped electrode in three dimensions with 29.9 mW cm^{-2} power output.

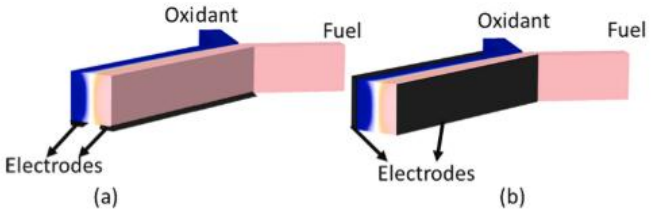

Figure 7. Flow-over electrode with (a) side-by-side streaming and (b) vertically-layered streaming. [26]

3.2.2 Flow-through electrode

In a flow-through configuration, reactant streams pass through a 3D porous electrode housing the catalytically active region. Mass transfer via diffusion/convection across these 3D electrodes replenishes the depletion layer, enhancing fuel utilization and power output. Kjeang et al. [122] demonstrated the porous electrodes can ensure the co-laminar flow phenomenon which significantly enhanced retention time for mass transfer and fuel utilization. Salloum et al. [123] conducted a study on a counter-flow and a sequential radial-flow system using porous flow-through electrodes. Recent studies have shown that the multi-layer construction approach is a powerful strategy for integrating porous flow-through electrodes, enabling enhanced structural control and performance. Krishnamurthy et al. [124] constructed a mathematical model that incorporates porous electrodes with flow-through capability resulted the power densities up to 193 mW cm^{-2}. Lee and Kjeang [82] employed a thin film current collector integrated into a chip and discovered that by optimizing the current collector design to reduce contact resistance, they could achieve a peak power density of 93 mW cm^{-2}. Li et al. [125] examined a vertically-layered that uses vanadium as fuel and has flow-through porous electrodes. In addition, Li et al. [126] examined a radial system with the similar electrode to overcome the size restrictions owing to longer active channel lengths [127]. With this configuration, the electrode size had little effect on the mixing region allowing the radial system to function at larger flow rates while keeping fuel utilisation. Wang et al. [128] conducted a computational and experimental investigation on a flow-through type, examining the behaviour of reactant species in co-laminar and counter-laminar flow configurations. The researchers discovered that the counter-laminar system displayed an uneven distribution of electric current and performed less effectively when compared to the co-laminar flow system. Salloum et al. [129] proposed a convective flow system incorporating porous disk electrodes, as illustrated in Figure 8. This configuration achieved an average OCV of 1.2 V, with peak current and power densities reaching 5.35 mA cm^{-2} and 2.8 mW cm^{-2}, respectively.

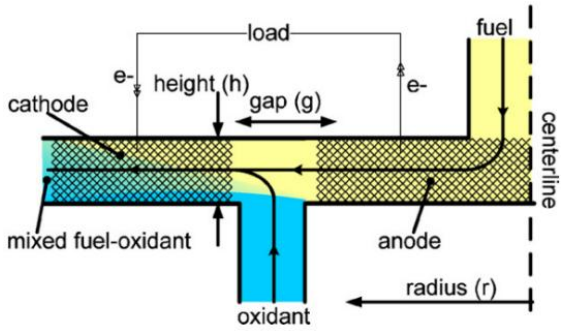

Figure 8. Flow over electrode [129]

3.2.3 Air-breathing electrode

Achieving moderate to high current density is only possible by using oxidants with greater solubility. Oxygen is an excellent choice as an oxidant due to its abundant availability in the environment. Nevertheless, it is low diffusivity that can constrain the mass transfer at cathode. Additionally, the oxygen concentration at a lower range of 2 - 4 mM is insufficient to generate a strong enough force to replenish the depleted region at the cathode [130]. Another conceptual with more inlets for boundary layer replenishment or fluids with a higher oxygen concentration may solve this limitation [131]. Therefore, this issue can be overcome by incorporating the open-air cathode system as shown in Figure 9. This allows for direct supply of oxygen from the air. This architecture is also utilised in conventional DMFC which are commonly referred to as open-air or air-breathing systems. The use of air-breathing electrodes effectively resolves many limitations in reactant mass transfer encountered when utilizing dissolved oxygen or other oxidants. Xuan et al. [132] examined the parameters that restrict the performance of air-breathing electrode system and explored if there is an adequate supply of oxygen from the surrounding air.

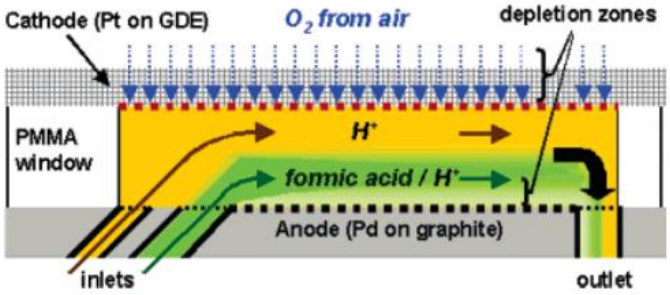

Figure 9. Air-breathing electrode [131]

Researchers have investigated novel electrode designs and methodologies to enhance the efficacy of DMFCs. A cylindrical anode system was introduced by Zhu et al. [133] through the use of a novel catalyst synthesis method. The authors emphasize that cylindrical anodes facilitate the scaling of fuel cell net power output. Furthermore, they examined the efficiency of cells and the properties of mass transfer in both acidic [133] and alkaline [134] electrolytes. Huizhi et al. [135] focused on modelling an air cathode and demonstrated that carefully regulating the electrolyte's hydrodynamic behavior can significantly lower internal transfer resistance.

The air-breathing system with an annular film [136] incorporates the principle of gas film cooling among numerous electrode combinations. A flow-over planar anode air-breathing system has been proposed to resolve the fuel transport limitation caused by the concentration boundary layer above the anode. To actively improve the depleted fuel region, Zhou et al. [137]

recommended the use of a fuel micro-jet. The comparison results indicated that the performance of an immersed fuel micro-jet was 40.9% better than that of the flow-over mode, resulting in an ideal power density of 119.3 mW cm^{-3}. It is imperative to employ standard-condition apparatus with comparable fuel/oxidant, flow rate, concentration, and other operating parameters in order to guarantee a fair comparison of power densities among various electrode types in membrane-less fuel cell systems. The impact of various electrode architectures on power density reported in the literature to date is illustrated in Figure 10, as provided by Tanveer et al. [26]. Table 8 shows the electrode configuration performance of membrane-less fuel cell from literature reviews.

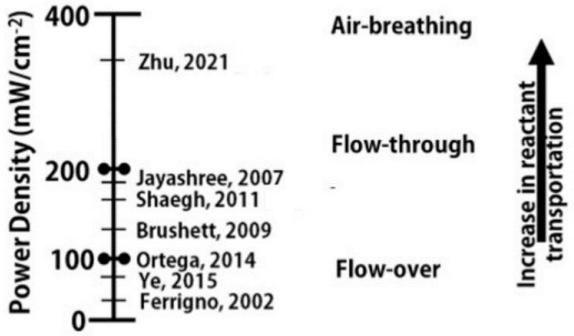

Figure 10. Comparative power density performance of different flow field architectures. [26]

Table 8. Electrode Architectures in Membrane-less Fuel Cells from literature reviews

Year	Ref	Electrode configuration	Study highlight	Results
2005	Choban et el. [59]	Flow-over	First demonstration of membraneless DMFC using co-laminar flow	Achieved power density ~45 μW cm^{-2} with graphite electrodes.
2008	Kjeang et al. [122]	Flow-through	Introduced porous electrodes with better mass transport.	3–4x power increase compared to flow-over; higher fuel utilization.
2015	Shyu et al. [138]	Air-breathing	Simplified design with passive air cathode.	Max power density of 1.23 mW cm^{-2} using methanol.
2020	Ortiz-Ortega [139]	Flow-through	The development of porous electrodes with a tunable Zn electrodeposit	Demonstrated a membraneless microfluidic Zn–air cell with flow-through electrodes, achieving high power densities.
2021	Tanveer et al. [140]	Flow-through	Proposed a membraneless microfluidic fuel cell with hollow flow channels and	Among the evaluated geometries, the hollow structure delivered the superior peak power density—exceeding that of the H-shaped, bridge-shaped, and rectangular

			porous flow-through electrodes.	channels by 6%, 18%, and a remarkable 82%, respectively.
2021	Ibáñez et al. [141]	Flow-over	Investigated diffusion and crossover issues.	Reduced cross-contamination through optimal flow control.
2023	Li et al. [142]	Flow-through	Used trapezoidal electrodes for counter-flow design.	The enhanced performance of the trapezoidal electrode is mainly due to the combined effect of a larger active surface area, lower ionic resistance, and improved fluid distribution.
2024	Liu et al. [143]	Air-breathing	Direct ammonia microfluidic cell with air cathode.	A peak power density of 8.43 mW cm^{-2} and a limiting current density of 78.58 mA cm^{-2} were achieved, exceeding the performance of most low-temperature ammonia fuel cells reported to date.

4.0 Challenges and opportunity

The path toward commercializing both conventional and membrane-less Direct Methanol Fuel Cells (DMFCs) is bottlenecked by distinct transport and manufacturing challenges that are fundamentally dictated by electrode architecture. For instance, while China successfully deployed a DMFC-powered logistics vehicle in 2019 [144], transitioning these systems to high-power applications remains economically and structurally challenging due to high noble metal dependencies and complex mass transport interfaces. In conventional CCS configurations, where the catalyst is deposited directly onto the GDL, non-uniform interfacial contact often necessitates excessively high noble metal loadings, typically exceeding 3 mg cm^{-2} or even 5 mg cm^{-2} Pt to compensate for poor catalyst utilization. Transitioning to a CCM architecture alters this paradigm by spraying the catalyst directly onto the polymer membrane which shortens proton transport pathways and enhances the triple-phase boundary. However, CCM architectures introduce severe mechanical and rheological challenges during fabrication. The localized swelling of the polymer membrane upon contact with liquid-ink solvents often leads to micro-cracking and delamination of the catalyst layer under subsequent thermal consolidation. To mitigate these structural defects, future research must shift from isolated fabrication techniques to integrated hybrid manufacturing strategies. Specifically, combining aspects of CCS and CCM, such as utilizing a dual-stage process that couples automated direct-spray deposition with automated decal transfer can optimize the gradient porosity of the electrode interface. This structural flexibility allows the electrode to adapt to dynamic volume changes under operation, unlocking superior mass-transport kinetics without compromising interfacial adhesion or requiring prohibitive Pt loadings.

Conversely, membrane-less fuel cell architectures completely eliminate the polymer membrane, shifting the primary technical bottleneck from material degradation to strict fluidic

boundary-layer management. Because these systems rely on a "virtual membrane" formed by co-laminar fluid dynamics, the electrode architecture serves as the direct physical determinant of both fluid stability and reactant utilization. Standard planar electrode architectures in microfluidic channels face severe trade-offs: increasing fluid velocities to minimize reactant crossover induces massive parasitic pressure drops across the stack, whereas slowing the flow causes rapid fuel depletion and boundary-layer breakdown. To overcome this, recent research has leveraged advanced microfabrication to transition toward 3D porous frameworks and flow-through architectures. While these high-surface-area topologies exponentially accelerate electrochemical kinetics, they cause critical architectural failure modes which intricate 3D porous electrodes can disrupt the laminar shear plane if the local permeability is non-uniform, causing premature fuel-oxidant mixing and catastrophic voltage loss. Besides, gaseous carbon dioxide bubbles generated at the anode tend to become pinned within highly tortuous porous networks. Without optimized gradient microchannel geometries, this gas entrapment blinds the reactive catalyst sites causing localized mass-transport starvation and electrolyte leakage. Consequently, unlocking the commercial scalability of membrane-less configurations requires a co-design approach where the internal porosity, pore tortuosity, and surface wettability of the 3D electrode architecture are systematically matched to the microchannel flow vectors to maintain laminar stability under dynamic load changes.

5.0 Industry and commercialization

The structural evolution of electrode architectures in both conventional and membrane-less DMFC directly dictates their viability for large-scale industrial deployment. Transitioning these systems from a laboratory setting to commercial market penetration requires shifting the analytical focus from isolated electrochemical performance metrics to systemic economic parameters, manufacturing scalability, and application-specific operating envelopes. The stark differences in the physical footprint and operational mechanics of conventional and membrane-less DMFC naturally divide their commercial trajectories into distinct market segments. Due to their robust structural containment and high volumetric power densities, conventional DMFCs are primary candidates for portable military power packs, auxiliary power units (APUs), and niche industrial logistics vehicles (e.g., forklifts and automated guided vehicles) [145,146]. For these applications, the industry requires electrode architectures that can withstand mechanical shock, vibration, and thousands of hours of start-stop cycling. Meanwhile, in membrane-less fuel cell system, the complete elimination of the physical membrane allows for extreme planar miniaturization and cost reduction. Consequently, membrane-less DMFC architectures are uniquely positioned to power micro-electromechanical systems (MEMS), remote environmental sensors, and single-use point-of-care diagnostic devices [146]. In these sub-watt applications, the primary commercial requirement is not extreme longevity, but shelf-life stability and low-cost fabrication.

For conventional configurations, scaling up CCM production requires replacing manual spraying with continuous roll-to-roll (R2R) slot-die coating. However, the industry faces an ongoing challenge: the mechanical stresses during R2R drying often induce micro-cracks in electrode architectures that feature high catalyst loadings. To achieve commercial continuity, future designs must integrate low-boiling-point solvents and binder-free, self-supporting 3D catalyst networks to ensure structural integrity during high-speed manufacturing. For membrane-less stacks, the core commercial bottleneck shifts from noble metal reduction to hydrodynamic scalability. While a single microfluidic channel operates reliably under strict laminar flow, scaling up to multi-cell industrial stacks requires distributing liquid fuel equally across hundreds of parallel microchannels. Minor variations in local electrode thickness or pore size distribution alter local hydraulic resistance, causing flow maldistribution, boundary-layer

breakdown, and severe fuel crossover. Therefore, commercialization is contingent upon developing high-precision injection molding or laser-ablation manufacturing methods capable of maintaining sub-micron tolerances across mass-produced electrode-channel assemblies [147].

Ultimately, industrial adoption must align with global sustainability initiatives, specifically UN Sustainable Development Goals for Affordable and Clean Energy (SDG 7) and Climate Action (SDG 13). Reaching this threshold requires an aggressive material transition toward earth-abundant, non-noble metal catalysts (such as transition metal oxides or nitrogen-doped carbon frameworks) embedded within recycled carbon-fiber substrate architectures [148]. Furthermore, an emerging commercial horizon involves exploring hybrid architectures that bridge the gap between both systems such as utilizing ultra-thin, highly porous inorganic separators within a microfluidic channel. This approach maintains the simplified, low-pressure plumbing of membrane-less configurations while providing a physical safeguard against crossover under dynamic load variations. By resolving these manufacturing and fluidic constraints through interdisciplinary collaboration, DMFC technologies can successfully transition from specialized academic subjects into commercially viable, sustainable energy solutions.

6.0 Conclusion

This review presents a comparative assessment of electrode development in conventional and membrane-less DMFC, emphasizing the operational principles, performance, and future prospects of each system. The MEA is a fundamental component of traditional DMFC, and it is typically CCS or CCM. The direct-spray method has emerged as a practicable fabrication approach due to its simplicity. On the other hand, membrane-less DMFCs establish a "virtual membrane" through co-laminar microfluidic flow, which eliminates the necessity for a physical membrane while still allowing for effective electrochemical separation. Electrode architecture serves as a pivotal determinant in governing the overall electrochemical performance and operational efficiency of fuel cell in both systems. In membrane-less configurations, electrodes are classified as flow-over, flow-through, and air-breathing types, with air-breathing electrodes exhibiting the most optimistic performance to date. In spite of this, the electrode fabrication process for membrane-less systems are still relatively unexplored and necessitates additional research to achieve optimal performance. Key challenges, including mechanical failure, long-term stability, and MEA durability, persist in impeding widespread implementation, despite substantial progress. Addressing these concerns is crucial for enhancing the operational reliability and longevity of the system. Ultimately, the advancement of electrode technologies in DMFCs is essential for the improvement of device performance and for the promotion of global sustainability initiatives, particularly SDG 7 (Affordable and Clean Energy) and SDG 13 (Climate Action) of the United Nations Sustainable Development Goals.

Acknowledgements

The authors gratefully acknowledge the financial support from The Ministry of Higher Education and University Kebangsaan Malaysia under Grant Number HiCoE (SelFuel): HiCoE -2023-001.

Author Contributions

The authors declare that they contributed equally to all stages of this manuscript and research.

Declaration of Competing Interest

The authors declare that they have no known competing financial interests or personal relationships that could have appeared to influence the work reported in this paper.

References

[1] National Renewable Energy Policy and Action Plan | ESCAP Policy Documents Managment n.d. https://policy.asiapacificenergy.org/node/1218 (accessed December 26, 2023).
[2] Yeo: Malaysia aiming for 20pc renewable energy use by 2025 | Malay Mail n.d. https://www.malaymail.com/news/malaysia/2019/09/03/yeo-malaysia-aiming-for-20pc-renewable-energy-use-by-2025/1786768 (accessed December 26, 2023).
[3] Osman SH, Kamarudin SK, Shaari N, Zakaria Z. Low-Temperature Fuel Cell Technology Development and Issues: An Overview. Arab J Sci Eng 2025. https://doi.org/10.1007/s13369-025-10045-9.
[4] Cacciola G, Antonucci V, Freni S. Technology up date and new strategies on fuel cells. J Power Sources 2001;100:67–79. https://doi.org/10.1016/S0378-7753(01)00884-9.
[5] Rao CRK, Trivedi DC. Chemical and electrochemical depositions of platinum group metals and their applications. Coord Chem Rev 2005;249:613–31. https://doi.org/10.1016/j.ccr.2004.08.015.
[6] Verma LK. Studies on methanol fuel cell. J Power Sources 2000;86:464–8. https://doi.org/10.1016/S0378-7753(99)00403-6.
[7] Hsieh C Te, Lin JY, Yang SY. Carbon nanotubes embedded with PtRu nanoparticles as methanol fuel cell electrocatalysts. Phys E Low-Dimensional Syst Nanostructures 2009;41:373–8. https://doi.org/10.1016/j.physe.2008.08.060.
[8] Osman SH, Kamarudin SK, Shaari N, Hanapi IH, Elham OSJ, Aminudin MA. Review on Direct Methanol Fuel Cells: Bridging the Gap between Theory and Application for Sustainable Energy Solutions. Energy and Fuels 2025. https://doi.org/10.1021/acs.energyfuels.4c05357.
[9] Porstmann S, Wannemacher T, Drossel W. A comprehensive comparison of state-of-the-art manufacturing methods for fuel cell bipolar plates including anticipated future industry trends. J Manuf Process 2020;60:366–83. https://doi.org/10.1016/j.jmapro.2020.10.041.
[10] Kjeang E, Djilali N, Sinton D. Microfluidic fuel cells: A review. J Power Sources 2009;186:353–69. https://doi.org/10.1016/j.jpowsour.2008.10.011.
[11] Goulet M-A, Kjeang E. Co-laminar flow cells for electrochemical energy conversion. J Power Sources 2014;260:186–96. https://doi.org/10.1016/j.jpowsour.2014.03.009.
[12] Esquivel JP, Buser JR, Lim CW, Domínguez C, Rojas S, Yager P, et al. Single-use paper-based hydrogen fuel cells for point-of-care diagnostic applications. J Power Sources 2017;342:442–51. https://doi.org/10.1016/j.jpowsour.2016.12.085.
[13] Abrego-Martínez JC, Moreno-Zuria A, Cuevas-Muñiz FM, Arriaga LG, Sun S, Mohamedi M. Design, fabrication and performance of a mixed-reactant membraneless micro direct methanol fuel cell stack. J Power Sources 2017;371:10–7. https://doi.org/10.1016/j.jpowsour.2017.10.026.

[14] Yeh E, Fu C, Hu L, Thakur R, Feng J, Lee LP. Self-powered integrated microfluidic point-of-care low-cost enabling (SIMPLE) chip 2017:1–12.
[15] Gajda I, Greenman J, Melhuish C, Ieropoulos I. Self-sustainable electricity production from algae grown in a microbial fuel cell system. Biomass and Bioenergy 2015;82:87–93. https://doi.org/10.1016/j.biombioe.2015.05.017.
[16] Zainoodin AM, Kamarudin SK, Daud WRW. Electrode in direct methanol fuel cells. Int J Hydrogen Energy 2010;35:4606–21. https://doi.org/10.1016/j.ijhydene.2010.02.036.
[17] Ramli ZAC, Shaari N, Saharuddin TST. Progress and major BARRIERS of nanocatalyst development in direct methanol fuel cell: A review. Int J Hydrogen Energy 2022;47:22114–46. https://doi.org/10.1016/j.ijhydene.2022.04.239.
[18] Ke Y, Yuan W, Liu Q, Zhou F, Guo W, Liu Z, et al. An overview of noncarbon support materials for membrane electrode assemblies in direct methanol fuel cells: Fundamental and applications. Mater Des 2023;233:112261. https://doi.org/10.1016/j.matdes.2023.112261.
[19] Jayakumar A, Madheswaran DK, Kumar NM. A critical assessment on functional attributes and degradation mechanism of membrane electrode assembly components in direct methanol fuel cells. Sustain 2021;13. https://doi.org/10.3390/su132413938.
[20] Zhang S, Jiang Y. Development of Membrane Electrode Assembly with Double-Catalytic Layer for Micro Direct Methanol Fuel Cell. Inventions 2024;9. https://doi.org/10.3390/inventions9010019.
[21] Halim EM, Chemchoub S, El Attar A, Salih FE, Oularbi L, EL RHAZI M. Recent Advances in Anode Metallic Catalysts Supported on Conducting Polymer-Based Materials for Direct Alcohol Fuel Cells. Front Energy Res 2022;10. https://doi.org/10.3389/fenrg.2022.843736.
[22] Gong L, Yang Z, Li K, Xing W, Liu C, Ge J. Recent development of methanol electrooxidation catalysts for direct methanol fuel cell. vol. 27. Elsevier B.V.; 2018.
[23] Wu B, Xu X, Dong G, Zhang M, Luo S, Leung DYC, et al. Computational modeling studies on microfluidic fuel cell: A prospective review. Renew Sustain Energy Rev 2024;191:114082. https://doi.org/10.1016/j.rser.2023.114082.
[24] Tanveer M, Ambreen T, Khan H, Man Kim G, Woo Park C. Paper-based microfluidic fuel cells and their applications: A prospective review. Energy Convers Manag 2022;264:115732. https://doi.org/10.1016/j.enconman.2022.115732.
[25] Wang Y, Luo S, Kwok HYH, Pan W, Zhang Y, Zhao X, et al. Microfluidic fuel cells with different types of fuels: A prospective review. Renew Sustain Energy Rev 2021;141:110806. https://doi.org/10.1016/j.rser.2021.110806.
[26] Tanveer M, Su Lim E, Kim KY. Effects of channel geometry and electrode architecture on reactant transportation in membraneless microfluidic fuel cells: A review. Fuel 2021;298:120818. https://doi.org/10.1016/j.fuel.2021.120818.
[27] Tanveer M, Kim KY. Flow configurations of membraneless microfluidic fuel cells: A review. Energies 2021;14. https://doi.org/10.3390/en14123381.
[28] Hanapi IH, Kamarudin SK, Zainoodin AM, Hasran UA. Membrane-less micro fuel cell system design and performance: An overview. Int J Energy Res 2019;43:8956–72. https://doi.org/10.1002/er.4804.
[29] Yu X, Manthiram A. Scalable Membraneless Direct Liquid Fuel Cells Based on a Catalyst-Selective Strategy. Energy Environ Mater 2018;1:13–9. https://doi.org/10.1002/eem2.12000.
[30] Goel S. From waste to watts in micro-devices: Review on development of Membraned and Membraneless Microfluidic Microbial Fuel Cell. Appl Mater Today 2018;11:270–9. https://doi.org/10.1016/j.apmt.2018.03.005.
[31] Bamgbopa MO, Almheiri S, Sun H. Prospects of recently developed membraneless cell designs for redox flow batteries. Renew Sustain Energy Rev 2017;70:506–18.

https://doi.org/10.1016/j.rser.2016.11.234.
[32] Bianchini C, Shen PK. Palladium-based electrocatalysts for alcohol oxidation in half cells and in direct alcohol fuel cells. Chem Rev 2009;109:4183–206. https://doi.org/10.1021/cr9000995.
[33] Dutta K, Kumar P, Das S, Kundu PP. Utilization of conducting polymers in fabricating polymer electrolyte membranes for application in direct methanol fuel cells. Polym Rev 2014;54:1–32. https://doi.org/10.1080/15583724.2013.839566.
[34] Ozoemena KI. Nanostructured platinum-free electrocatalysts in alkaline direct alcohol fuel cells: Catalyst design, principles and applications. RSC Adv 2016;6:89523–50. https://doi.org/10.1039/c6ra15057h.
[35] Cai W, Fan K, Li J, Ma L, Xu G, Xu S, et al. A bi-functional polymeric nano-sieve Nafion composite membrane: Improved performance for direct methanol fuel cell applications. Int J Hydrogen Energy 2016;41:17102–11. https://doi.org/10.1016/j.ijhydene.2016.07.128.
[36] Xu X, Wang H, Lu S, Peng S, Xiang Y. A phosphotungstic acid self-anchored hybrid proton exchange membrane for direct methanol fuel cells. RSC Adv 2016;6:43049–55. https://doi.org/10.1039/c6ra07318b.
[37] You PY, Kamarudin SK, Masdar MS. Improved performance of sulfonated polyimide composite membranes with rice husk ash as a bio-filler for application in direct methanol fuel cells. Int J Hydrogen Energy 2019;44:1857–66. https://doi.org/10.1016/j.ijhydene.2018.11.166.
[38] Berretti E, Osmieri L, Baglio V, Miller HA, Filippi J, Vizza F, et al. Direct Alcohol Fuel Cells: A Comparative Review of Acidic and Alkaline Systems. vol. 6. Springer Nature Singapore; 2023. https://doi.org/10.1007/s41918-023-00189-3.
[39] Vecchio C Lo, Lyu X, Gatto I, Zulevi B, Serov A, Baglio V. Performance investigation of alkaline direct methanol fuel cell with commercial PGM-free cathodic materials. J Power Sources 2023;561:1–6. https://doi.org/10.1016/j.jpowsour.2023.232732.
[40] Antolini E, Gonzalez ER. Alkaline direct alcohol fuel cells. J Power Sources 2010;195:3431–50. https://doi.org/10.1016/j.jpowsour.2009.11.145.
[41] Papadias DD, Ahluwalia RK, Thomson JK, Meyer HM, Brady MP, Wang H, et al. Degradation of SS316L bipolar plates in simulated fuel cell environment: Corrosion rate, barrier film formation kinetics and contact resistance. J Power Sources 2015;273:1237–49. https://doi.org/10.1016/j.jpowsour.2014.02.053.
[42] Hren M, Božič M, Fakin D, Kleinschek KS, Gorgieva S. Alkaline membrane fuel cells: Anion exchange membranes and fuels. Sustain Energy Fuels 2021;5:604–37. https://doi.org/10.1039/d0se01373k.
[43] Rizo R, Arán-Ais RM, Padgett E, Muller DA, Lázaro MJ, Solla-Gullón J, et al. Pt-Richcore/Sn-Richsubsurface/Ptskin Nanocubes As Highly Active and Stable Electrocatalysts for the Ethanol Oxidation Reaction. J Am Chem Soc 2018;140:3791–7. https://doi.org/10.1021/jacs.8b00588.
[44] Li W, Fang J, Lv M, Chen C, Chi X, Yang Y, et al. Novel anion exchange membranes based on polymerizable imidazolium salt for alkaline fuel cell applications. J Mater Chem 2011;21:11340–6. https://doi.org/10.1039/c1jm11093d.
[45] Ye YS, Cheng MY, Xie XL, Rick J, Huang YJ, Chang FC, et al. Alkali doped polyvinyl alcohol/graphene electrolyte for direct methanol alkaline fuel cells. J Power Sources 2013;239:424–32. https://doi.org/10.1016/j.jpowsour.2013.03.021.
[46] Sajjad SD, Liu D, Wei Z, Sakri S, Shen Y, Hong Y, et al. Guanidinium based blend anion exchange membranes for direct methanol alkaline fuel cells (DMAFCs). J Power Sources 2015;300:95–103. https://doi.org/10.1016/j.jpowsour.2015.08.002.
[47] Gupta UK, Pramanik H. Electrooxidation study of pure ethanol/methanol and their mixture for the application in direct alcohol alkaline fuel cells (DAAFCs). Int J Hydrogen

Energy 2019:421–35. https://doi.org/10.1016/j.ijhydene.2018.03.008.
[48] Varcoe JR, Slade RCT, Yee ELH, Poynton SD, Driscoll DJ. Investigations into the ex situ methanol, ethanol and ethylene glycol permeabilities of alkaline polymer electrolyte membranes. J Power Sources 2007;173:194–9. https://doi.org/10.1016/j.jpowsour.2007.04.068.
[49] Burhan H, Cellat K, Yılmaz G, Şen F. Investigation of Fumasep® FAA3-50 Membranes in Alkaline Direct Methanol Fuel Cells Carmelo. Direct Liq Fuel Cells Fundam Adv Futur 2020:71–94. https://doi.org/10.1016/B978-0-12-818624-4.00003-0.
[50] Zakaria Z, Shaari N, Kamarudin SK. Preliminary Study of Alkaline Direct Ethanol Fuel Cell by using Crosslinked Quaternized Poly (Vinyl Alcohol)/Graphene Oxide Membrane. J Kejuruter 2018;30:219–27. https://doi.org/10.17576/jkukm-2018-30(2)-12.
[51] Shaari N, Kamarudin SK, Zakaria Z. Enhanced alkaline stability and performance of alkali-doped quaternized poly(vinyl alcohol) membranes for passive direct ethanol fuel cell. Int J Energy Res 2019;43:5252–65. https://doi.org/10.1002/er.4513.
[52] Nguyen N-T, Wereley ST, House A. Fundamentals and Applications of Microfluidics - Second Edition. 2002.
[53] Whitesides GM. The origins and the future of microfluidics. Nature 2006;442:368–73. https://doi.org/10.1038/nature05058.
[54] Petrovic S, Hossain E. Development of a Novel Technological Readiness Assessment Tool for Fuel Cell Technology. IEEE Access 2020;8:132237–52. https://doi.org/10.1109/ACCESS.2020.3009193.
[55] Choban E. Microfluidic fuel cell based on laminar flow. J Power Sources 2004;128:54–60. https://doi.org/10.1016/j.jpowsour.2003.11.052.
[56] Ha S-M, Ahn Y. Laminar flow-based micro fuel cell utilizing grooved electrode surface. J Power Sources 2014;267:731–8. https://doi.org/10.1016/j.jpowsour.2014.06.005.
[57] Hanapi IH, Kamarudin SK, Zainoodin AM, Hasran UA. Optimization of Multiple Reactants in a Membrane-Less Direct Methanol Fuel Cell (DMFC) 2023:1–20.
[58] Cohen JL, Westly DA, Pechenik A, Abruña HD. Fabrication and preliminary testing of a planar membraneless microchannel fuel cell. J Power Sources 2005;139:96–105. https://doi.org/10.1016/j.jpowsour.2004.06.072.
[59] Choban ER, Spendelow JS, Gancs L, Wieckowski A, Kenis PJA. Membraneless laminar flow-based micro fuel cells operating in alkaline, acidic, and acidic/alkaline media. Electrochim Acta 2005;50:5390–8. https://doi.org/10.1016/j.electacta.2005.03.019.
[60] Ponmani K, Durga S, Arun A, Kiruthika S, Muthukumaran B. Development of Membraneless Sodium Perborate Fuel Cell for Media Flexible Power Generation. Int J Electrochem 2014;2014:1–9. https://doi.org/10.1155/2014/962161.
[61] Rathoure AK, Pramanik H. Electrooxidation study of methanol using H 2 O 2 and air as mixed oxidant at cathode in air breathing microfluidic fuel cell. Int J Hydrogen Energy 2016;41:15287–94. https://doi.org/10.1016/j.ijhydene.2016.07.058.
[62] Chen F, Chang MH, Hsu CW. Analysis of membraneless microfuel cell using decomposition of hydrogen peroxide in a Y-shaped microchannel. Electrochim Acta 2007;52:7270–7. https://doi.org/10.1016/j.electacta.2007.05.072.
[63] Rahim AHA, Salami A, Kamarudin SK, Hanapi S. An overview of polymer electrolyte membrane electrolyzer for hydrogen production : Modeling and mass transport. J Power Sources 2016;309:56–65. https://doi.org/10.1016/j.jpowsour.2016.01.012.
[64] Chen Z, Cao J, Chen Z, Xu J, Wang W. Mesoporous carbon synthesized from dual colloidal silica/block copolymer template approach as the support of platinum nanoparticles for direct methanol fuel cells. Electrochim Acta 2013;88:184–92. https://doi.org/10.1016/j.electacta.2012.10.030.
[65] Jha N, Jafri RI, Rajalakshmi N, Ramaprabhu S. Graphene-multi walled carbon

nanotube hybrid electrocatalyst support material for direct methanol fuel cell. Int J Hydrogen Energy 2011;36:7284–90. https://doi.org/10.1016/j.ijhydene.2011.03.008.
[66] Kanninen P, Borghei M, Sorsa O, Pohjalainen E, Kauppinen EI, Ruiz V, et al. Highly efficient cathode catalyst layer based on nitrogen-doped carbon nanotubes for the alkaline direct methanol fuel cell. Appl Catal B Environ 2014;156–157:341–9. https://doi.org/10.1016/j.apcatb.2014.03.041.
[67] Borghei M, Scotti G, Kanninen P, Weckman T, Anoshkin I V., Nasibulin AG, et al. Enhanced performance of a silicon microfabricated direct methanol fuel cell with PtRu catalysts supported on few-walled carbon nanotubes. Energy 2014;65:612–20. https://doi.org/10.1016/j.energy.2013.11.067.
[68] Deng H, Zhang Y, Zheng X, Li Y, Zhang X, Liu X. A CNT (carbon nanotube) paper as cathode gas diffusion electrode for water management of passive μ-DMFC (micro-direct methanol fuel cell) with highly concentrated methanol. Energy 2015;82:236–41. https://doi.org/10.1016/j.energy.2015.01.034.
[69] Bruno MM, Viva FA, Petruccelli MA, Corti HR. Platinum supported on mesoporous carbon as cathode catalyst for direct methanol fuel cells. J Power Sources 2015;278:458–63. https://doi.org/10.1016/j.jpowsour.2014.12.097.
[70] Kang YS, Jung N, Choi KH, Lee MJ, Ahn M, Cho YH, et al. Anode electrode with carbon buffer layer for improving methanol oxidation reaction in direct methanol fuel cell. Appl Surf Sci 2014;290:246–51. https://doi.org/10.1016/j.apsusc.2013.11.059.
[71] Zainoodin AM, Kamarudin SK, Masdar MS, Daud WRW, Mohamad AB, Sahari J. High power direct methanol fuel cell with a porous carbon nanofiber anode layer. Appl Energy 2014;113:946–54. https://doi.org/10.1016/j.apenergy.2013.07.066.
[72] Yan XH, Wu R, Xu JB, Luo Z, Zhao TS. A monolayer graphene - Nafion sandwich membrane for direct methanol fuel cells. J Power Sources 2016;311:188–94. https://doi.org/10.1016/j.jpowsour.2016.02.030.
[73] Schlange A, Dos Santos AR, Hasse B, Etzold BJM, Kunz U, Turek T. Titanium carbide-derived carbon as a novel support for platinum catalysts in direct methanol fuel cell application. J Power Sources 2012;199:22–8. https://doi.org/10.1016/j.jpowsour.2011.09.107.
[74] Yuan T, Yang J, Wang Y, Ding H, Li X, Liu L, et al. Anodic diffusion layer with graphene-carbon nanotubes composite material for passive direct methanol fuel cell. Electrochim Acta 2014;147:265–70. https://doi.org/10.1016/j.electacta.2014.09.124.
[75] Rambabu G, Bhat SD. Sulfonated fullerene in SPEEK matrix and its impact on the membrane electrolyte properties in direct methanol fuel cells. Electrochim Acta 2015;176:657–69. https://doi.org/10.1016/j.electacta.2015.07.045.
[76] Morales-Acosta D, Morales-Acosta MD, Godinez LA, Álvarez-Contreras L, Duron-Torres SM, Ledesma-García J, et al. PdCo supported on multiwalled carbon nanotubes as an anode catalyst in a microfluidic formic acid fuel cell. J Power Sources 2011;196:9270–5. https://doi.org/10.1016/j.jpowsour.2011.07.064.
[77] Salloum KS, Posner JD. A membraneless microfluidic fuel cell stack. J Power Sources 2011;196:1229–34. https://doi.org/10.1016/j.jpowsour.2010.08.069.
[78] Gago AS, Morales-Acosta D, Arriaga LG, Alonso-Vante N. Carbon supported ruthenium chalcogenide as cathode catalyst in a microfluidic formic acid fuel cell. J Power Sources 2011;196:1324–8. https://doi.org/10.1016/j.jpowsour.2010.08.109.
[79] Brushett FR, Naughton MS, Ng JWD, Yin L, Kenis PJA. Analysis of Pt/C electrode performance in a flowing-electrolyte alkaline fuel cell. Int J Hydrogen Energy 2012;37:2559–70. https://doi.org/10.1016/j.ijhydene.2011.10.078.
[80] López-Montesinos PO, Yossakda N, Schmidt A, Brushett FR, Pelton WE, Kenis PJA. Design, fabrication, and characterization of a planar, silicon-based, monolithically integrated micro laminar flow fuel cell with a bridge-shaped microchannel cross-section. J Power Sources

2011;196:4638–45. https://doi.org/10.1016/j.jpowsour.2011.01.037.
[81] Moore S, Sinton D, Erickson D. A plate-frame flow-through microfluidic fuel cell stack. J Power Sources 2011;196:9481–7. https://doi.org/10.1016/j.jpowsour.2011.07.024.
[82] Lee JW, Kjeang E. Chip-embedded thin film current collector for microfluidic fuel cells. Int J Hydrogen Energy 2012;37:9359–67. https://doi.org/10.1016/j.ijhydene.2012.02.155.
[83] Lee JW, Hong JK, Kjeang E. Electrochemical characteristics of vanadium redox reactions on porous carbon electrodes for microfluidic fuel cell applications. Electrochim Acta 2012;83:430–8. https://doi.org/10.1016/j.electacta.2012.07.104.
[84] Mousavi Shaegh SA, Nguyen N-T, Chan SH. Air-breathing microfluidic fuel cell with fuel reservoir. J Power Sources 2012;209:312–7. https://doi.org/10.1016/j.jpowsour.2012.02.115.
[85] Jindal A, Basu S, Chauhan N, Ukai T, Kumar DS, Samudhyatha KT. Application of electrospun CNxnanofibers as cathode in microfluidic fuel cell. J Power Sources 2017;342:165–74. https://doi.org/10.1016/j.jpowsour.2016.12.047.
[86] Shahgaldi S, Alaefour I, Li X. Impact of manufacturing processes on proton exchange membrane fuel cell performance. Appl Energy 2018;225:1022–32. https://doi.org/10.1016/j.apenergy.2018.05.086.
[87] Shahgaldi S, Zhao J, Alaefour I, Li X. Investigation of catalytic vs reactant transport effect of catalyst layers on proton exchange membrane fuel cell performance. Fuel 2017;208:321–8. https://doi.org/10.1016/j.fuel.2017.07.035.
[88] Martin S, Garcia-Ybarra PL, Castillo JL. Long-term operation of a proton exchange membrane fuel cell without external humidification. Appl Energy 2017;205:1012–20. https://doi.org/10.1016/j.apenergy.2017.08.157.
[89] Chun YG, Kim CS, Peck DH, Shin DR. Performance of a polymer electrolyte membrane fuel cell with thin film catalyst electrodes. J Power Sources 1998;71:174–8. https://doi.org/10.1016/S0378-7753(97)02792-4.
[90] Lee HK, Park JH, Kim DY, Lee TH. A study on the characteristics of the diffusion layer thickness and porosity of the PEMFC. J Power Sources 2004;131:200–6. https://doi.org/10.1016/j.jpowsour.2003.12.039.
[91] Kim CS, Chun YG, Peck DH, Shin DR. A novel process to fabricate membrane electrode assemblies for proton exchange membrane fuel cells. Int J Hydrogen Energy 1998;23:1045–8. https://doi.org/10.1016/S0360-3199(98)00021-4.
[92] Lee E, Kim DH, Pak C. Effects of cathode catalyst layer fabrication parameters on the performance of high-temperature polymer electrolyte membrane fuel cells. Appl Surf Sci 2020;510:145461. https://doi.org/10.1016/j.apsusc.2020.145461.
[93] Gallo Stampino P, Cristiani C, Dotelli G, Omati L, Zampori L, Pelosato R, et al. Effect of different substrates, inks composition and rheology on coating deposition of microporous layer (MPL) for PEM-FCs. Catal Today 2009;147:30–5. https://doi.org/10.1016/j.cattod.2009.07.023.
[94] Achmad F, Kamarudin SK, Daud WRW, Majlan EH. Passive direct methanol fuel cells for portable electronic devices. Appl Energy 2011;88:1681–9. https://doi.org/10.1016/j.apenergy.2010.11.012.
[95] Zainoodin AM, Tsujiguchi T, Masdar MS, Kamarudin SK, Osaka Y, Kodama A. Performance of a direct formic acid fuel cell fabricated by ultrasonic spraying. Int J Hydrogen Energy 2018;43:6413–20. https://doi.org/10.1016/j.ijhydene.2018.02.024.
[96] Fofana D, Natarajan SK, Hamelin J, Benard P. Low platinum, high limiting current density of the PEMFC (proton exchange membrane fuel cell) based on multilayer cathode catalyst approach. Energy 2014;64:398–403. https://doi.org/10.1016/j.energy.2013.10.021.
[97] Kim GH, Eom KS, Kim MJ, Yoo SJ, Jang JH, Kim HJ, et al. Design of an Advanced

Membrane Electrode Assembly Employing a Double-Layered Cathode for a PEM Fuel Cell. ACS Appl Mater Interfaces 2015;7:27581–5. https://doi.org/10.1021/acsami.5b07346.
[98] Shahgaldi S, Alaefour I, Li X. The impact of short side chain ionomer on polymer electrolyte membrane fuel cell performance and durability. Appl Energy 2018;217:295–302. https://doi.org/10.1016/j.apenergy.2018.02.154.
[99] Wang S, Shang Y, Wang Y, Wang J. Fabrication and electrochemical performance of Poly (2,5-benzimidazole) (ABPBI)-based MEA by catalyst coated membrane (CCM) method for high-temperature polymer electrolyte fuel cells. Int J Hydrogen Energy 2013;38:11060–6. https://doi.org/10.1016/j.ijhydene.2013.01.102.
[100] Liang H, Su H, Pollet BG, Linkov V, Pasupathi S. Membrane electrode assembly with enhanced platinum utilization for high temperature proton exchange membrane fuel cell prepared by catalyst coating membrane method. J Power Sources 2014;266:107–13. https://doi.org/10.1016/j.jpowsour.2014.05.014.
[101] Liang H, Su H, Pollet BG, Pasupathi S. Development of membrane electrode assembly for high temperature proton exchange membrane fuel cell by catalyst coating membrane method. J Power Sources 2015;288:121–7. https://doi.org/10.1016/j.jpowsour.2015.04.123.
[102] Hu M, Sui S, Zhu X, Yu Q, Cao G, Hong X, et al. A 10 kW class PEM fuel cell stack based on the catalyst-coated membrane (CCM) method. Int J Hydrogen Energy 2006;31:1010–8. https://doi.org/10.1016/j.ijhydene.2006.02.018.
[103] Hnát J, Plevova M, Tufa RA, Zitka J, Paidar M, Bouzek K. Development and testing of a novel catalyst-coated membrane with platinum-free catalysts for alkaline water electrolysis. Int J Hydrogen Energy 2019;44:17493–504. https://doi.org/10.1016/j.ijhydene.2019.05.054.
[104] Tang H, Wang S, Jiang SP, Pan M. A comparative study of CCM and hot-pressed MEAs for PEM fuel cells. J Power Sources 2007;170:140–4. https://doi.org/10.1016/j.jpowsour.2007.03.062.
[105] Sadeghi Alavijeh A, Khorasany RMH, Habisch A, Wang GG, Kjeang E. Creep properties of catalyst coated membranes for polymer electrolyte fuel cells. J Power Sources 2015;285:16–28. https://doi.org/10.1016/j.jpowsour.2015.03.082.
[106] Zhang J. PEM fuel cell electrocatalysts and catalyst layers: Fundamentals and applications. 2008. https://doi.org/10.1007/978-1-84800-936-3.
[107] Song SQ, Liang ZX, Zhou WJ, Sun GQ, Xin Q, Stergiopoulos V, et al. Direct methanol fuel cells: The effect of electrode fabrication procedure on MEAs structural properties and cell performance. J Power Sources 2005;145:495–501. https://doi.org/10.1016/j.jpowsour.2005.02.069.
[108] Sarkar J, Bhattacharyya S. Application of graphene and graphene-based materials in clean energy-related devices Minghui. Arch Thermodyn 2012;33:23–40. https://doi.org/10.1002/er.
[109] Li Y, Fu Z, Li Y, Zhang G. A Comparative Study of CCM and CCS Membrane Electrode Assemblies for High-Temperature Proton Exchange Membrane Fuel Cells with a CsH5(PO4)2-Doped Polybenzimidazole Membrane. Materials (Basel) 2023;16. https://doi.org/10.3390/ma16113925.
[110] Rohendi D, Syarif N, Said M, Utami MT, Marcelina Y. Utilization of catalyst-coated membrane (CCM) and spraying methods in fabrication membrane electrode assembly (MEA) for direct methanol fuel Cell (DMFC) using Pt-Co / C catalyst. J Phys Conf Ser 2019;1282. https://doi.org/10.1088/1742-6596/1282/1/012065.
[111] Mauger SA, Wang M, Cetinbas FC, Dzara MJ, Park J, Myers DJ, et al. Development of high-performance roll-to-roll-coated gas-diffusion-electrode-based fuel cells. J Power Sources 2021;506:230039. https://doi.org/10.1016/j.jpowsour.2021.230039.
[112] Breitwieser M, Klingele M, Vierrath S, Zengerle R, Thiele S. Tailoring the Membrane-

Electrode Interface in PEM Fuel Cells: A Review and Perspective on Novel Engineering Approaches. Adv Energy Mater 2018;8. https://doi.org/10.1002/aenm.201701257.
[113] Jinnouchi R, Kudo K, Kodama K, Kitano N, Suzuki T, Minami S, et al. The role of oxygen-permeable ionomer for polymer electrolyte fuel cells. Nat Commun 2021;12. https://doi.org/10.1038/s41467-021-25301-3.
[114] Lee CH, Kort-Kamp WJM, Yu H, Cullen DA, Patterson BM, Arman TA, et al. Grooved electrodes for high-power-density fuel cells. Nat Energy 2023;8:685–94. https://doi.org/10.1038/s41560-023-01263-2.
[115] Mousavi Shaegh SA, Nguyen NT, Chan SH. A review on membraneless laminar flow-based fuel cells. Int J Hydrogen Energy 2011;36:5675–94. https://doi.org/10.1016/j.ijhydene.2011.01.063.
[116] Ferrigno R, Stroock AD, Clark TD, Mayer M, Whitesides GM. Membraneless Vanadium Redox Fuel Cell Using Laminar Flow. J Am Chem Soc 2002;124:12930–1. https://doi.org/10.1021/ja020812q.
[117] Tominaka S, Obata H, Osaka T. On-chip direct methanol fuel cells of a monolithic design: Consideration on validity of active-type system. Energy Environ Sci 2009;2:845–8. https://doi.org/10.1039/b904339j.
[118] Maynard HL, Meyers JP. Miniature fuel cells for portable power: Design considerations and challenges. J Vac Sci Technol B Microelectron Nanom Struct Process Meas Phenom 2002;20:1287–97. https://doi.org/10.1116/1.1488641.
[119] Sun MH, Velve Casquillas G, Guo SS, Shi J, Ji H, Ouyang Q, et al. Characterization of microfluidic fuel cell based on multiple laminar flow. Microelectron Eng 2007;84:1182–5. https://doi.org/10.1016/j.mee.2007.01.175.
[120] Mota N Da, Finkelstein DA, Kirtland JD, Rodriguez CA, Stroock AD, Abruña HD. Membraneless, room-temperature, direct borohydride/cerium fuel cell with power density of over 0.25 W/cm 2. J Am Chem Soc 2012;134:6076–9. https://doi.org/10.1021/ja211751k.
[121] Liu Z, Ye D, Chen R, Zhang B, Zhu X, Liao Q. A dual-functional three-dimensional herringbone-like electrode for a membraneless microfluidic fuel cell. J Power Sources 2019;438:227058. https://doi.org/10.1016/j.jpowsour.2019.227058.
[122] Kjeang E, Michel R, Harrington DA, Djilali N, Sinton D. A microfluidic fuel cell with flow-through porous electrodes. J Am Chem Soc 2008;130:4000–6. https://doi.org/10.1021/ja078248c.
[123] Salloum KS, Posner JD. Counter flow membraneless microfluidic fuel cell. J Power Sources 2010;195:6941–4. https://doi.org/10.1016/j.jpowsour.2010.03.096.
[124] Krishnamurthy D, Johansson EO, Lee JW, Kjeang E. Computational modeling of microfluidic fuel cells with flow-through porous electrodes. J Power Sources 2011;196:10019–31. https://doi.org/10.1016/j.jpowsour.2011.08.024.
[125] Li L, Nikiforidis G, Leung MKH, Daoud WA. Vanadium microfluidic fuel cell with novel multi-layer flow-through porous electrodes: Model, simulations and experiments. Appl Energy 2016;177:729–39. https://doi.org/10.1016/j.apenergy.2016.05.072.
[126] Li L, Bei S, Liu R, Xu Q, Zheng K, She Y, et al. Design of a radial vanadium redox microfluidic fuel cell: A new way to break the size limitation. Int J Energy Res 2019;43:3028–37. https://doi.org/10.1002/er.4473.
[127] Tanveer M, Kim KY. Performance analysis of microfluidic fuel cells with various inlet locations and multiple compartments. Energy Convers Manag 2018;166:328–36. https://doi.org/10.1016/j.enconman.2018.04.043.
[128] Wang Y, Leung DYC, Zhang H, Xuan J, Wang H. Numerical and experimental comparative study of microfluidic fuel cells with different flow configurations: Co-flow vs. counter-flow cell. Appl Energy 2017;203:535–48. https://doi.org/10.1016/j.apenergy.2017.06.070.

[129] Salloum KS, Hayes JR, Friesen CA, Posner JD. Sequential flow membraneless microfluidic fuel cell with porous electrodes. J Power Sources 2008;180:243–52. https://doi.org/10.1016/j.jpowsour.2007.12.116.
[130] Zhang B, Ye D, Li J, Zhu X, Liao Q. Electrodeposition of Pd catalyst layer on graphite rod electrodes for direct formic acid oxidation. J Power Sources 2012;214:277–84. https://doi.org/10.1016/j.jpowsour.2012.04.007.
[131] Jayashree RS, Gancs L, Choban ER, Primak A, Natarajan D, Markoski LJ, et al. Air-Breathing Laminar Flow-Based Microfluidic Fuel Cell. J Am Chem Soc 2005;127:16758–9. https://doi.org/10.1021/ja054599k.
[132] Xuan J, Leung DYC, Wang H, Leung MKH, Wang B, Ni M. Air-breathing membraneless laminar flow-based fuel cells: Do they breathe enough oxygen? Appl Energy 2013;104:400–7. https://doi.org/10.1016/j.apenergy.2012.10.063.
[133] Zhu X, Zhang B, Ye DD, Li J, Liao Q. Air-breathing direct formic acid microfluidic fuel cell with an array of cylinder anodes. J Power Sources 2014;247:346–53. https://doi.org/10.1016/j.jpowsour.2013.08.119.
[134] Ye DD, Zhang B, Zhu X, Sui PC, Djilali N, Liao Q. Computational modeling of alkaline air-breathing microfluidic fuel cells with an array of cylinder anodes. J Power Sources 2015;288:150–9. https://doi.org/10.1016/j.jpowsour.2015.04.087.
[135] Wang H, Leung DYC, Xuan J. Modeling of an air cathode for microfluidic fuel cells: Transport and polarization behaviors. Int J Hydrogen Energy 2011;36:14704–18. https://doi.org/10.1016/j.ijhydene.2011.08.033.
[136] Zhu X, Zhou Y, Ye D-D, Chen R, Zhang T, Liao Q. Discrete-holes film fueling anode heads for high performance air-breathing microfluidic fuel cell. J Power Sources 2021;482:228966. https://doi.org/10.1016/j.jpowsour.2020.228966.
[137] Zhou Y, Zhang B, Zhu X, Ye DD, Chen R, Zhang T, et al. Enhancing fuel transport in air-breathing microfluidic fuel cells by immersed fuel micro-jet. J Power Sources 2020;445:227326. https://doi.org/10.1016/j.jpowsour.2019.227326.
[138] Shyu JC, Wang PY, Lee CL, Chang SC, Sheu TS, Kuo CH, et al. Fabrication and test of an air-breathing microfluidic fuel cell. Energies 2015;8:2082–96. https://doi.org/10.3390/en8032082.
[139] Ortiz-Ortega E, Díaz-Patiño L, Bejar J, Trejo G, Guerra-Balcázar M, Espinosa-Magaña F, et al. A Flow-Through Membraneless Microfluidic Zinc-Air Cell. ACS Appl Mater Interfaces 2020;12:41185–99. https://doi.org/10.1021/acsami.0c08525.
[140] Tanveer M, Kim KY. A membraneless microfluidic fuel cell with a hollow flow channel and porous flow-through electrodes. Int J Energy Res 2021;45:8536–50. https://doi.org/10.1002/er.6390.
[141] Ibáñez SE, Quintero AE, García-Salaberri PA, Vera M. Effects of the diffusive mixing and self-discharge reactions in microfluidic membraneless vanadium redox flow batteries. Int J Heat Mass Transf 2021;170:121022. https://doi.org/10.1016/j.ijheatmasstransfer.2021.121022.
[142] Li L, Ling L, Xie Y, Shan S, Bei S, Zheng K, et al. Counter-flow microfluidic fuel cell with trapezoidal electrodes. Sustain Energy Technol Assessments 2023;56. https://doi.org/10.1016/j.seta.2022.103005.
[143] Liu H, Xu Y, Zhang S, Zhou Y, Liu N, Liu J, et al. High cost-performance direct ammonia microfluidic fuel cell benefited from nickel nanoparticle anode and catalyst-free cathode. Int J Hydrogen Energy 2024;69:1417–25. https://doi.org/10.1016/j.ijhydene.2024.05.160.
[144] China: Yuantong Debuts A Direct Methanol Fuel Cell Logistics Vehicle - FuelCellsWorks n.d. https://fuelcellsworks.com/news/china-yuantong-debuts-a-direct-methanol-fuel-cell-logistics-vehicle/ (accessed January 28, 2024).

[145] Romagnoli M, Testa V, Romagnoli M, Testa V. Perspective Chapter: Methanol as a Fuel for Direct Methanol Fuel Cells (DMFCs) – Principles and Performance. Methanol Fuel Transp Sect Fuel Cells 2023. https://doi.org/10.5772/INTECHOPEN.1002872.
[146] Lo Vecchio C, Serov A, Dicome M, Zulevi B, Aricò AS, Baglio V. Investigating the durability of a direct methanol fuel cell equipped with commercial Platinum Group Metal-free cathodic electro-catalysts. Electrochim Acta 2021;394. https://doi.org/10.1016/J.ELECTACTA.2021.139108.
[147] Liu X, Fan K, Huang X, Ge J, Liu Y, Kang H. Recent advances in artificial intelligence boosting materials design for electrochemical energy storage. Chem Eng J 2024;490. https://doi.org/10.1016/J.CEJ.2024.151625.
[148] Arora NK, Mishra I. Sustainable development goal 13: recent progress and challenges to climate action. Environ Sustain 2023;6:297–301. https://doi.org/10.1007/S42398-023-00287-4.